STATE ESTIMATION BASED FAULT LOCATION USING PMU MEASUREMENTS

A THESIS SUBMITTED TO
THE GRADUATE SCHOOL OF NATURAL AND APPLIED SCIENCES
OF
MIDDLE EAST TECHNICAL UNIVERSITY

BY

AHMET ÖNER

IN PARTIAL FULFILLMENT OF THE REQUIREMENTS
FOR
THE DEGREE OF MASTER OF SCIENCE
IN
ELECTRICAL AND ELECTRONICS ENGINEERING

JULY 2016

Approval of the thesis:

STATE ESTIMATION BASED FAULT LOCATION USING PMU MEASUREMENTS

submitted by **AHMET ÖNER** in partial fulfillment of the requirements for the degree of **Master of Science in Electrical and Electronics Engineering Department, Middle East Technical University** by,

Prof. Dr. Gülbin Dural Ünver _____
Dean, Graduate School of **Natural and Applied Sciences**

Prof. Dr. Gönül Turhan Sayan _____
Head of Department, **Electrical and Electronics Engineering**

Assist. Prof. Dr. Murat Göl _____
Supervisor, **Electrical and Electronics Eng. Dept., METU**

Examining Committee Members:

Prof. Dr. Nezih Güven _____
Electrical and Electronics Engineering Dept., METU

Assist. Prof. Dr. Murat Göl _____
Electrical and Electronics Engineering Dept., METU

Assoc. Prof. Dr. Özgül Salor Durna _____
Electrical and Electronics Engineering Dept., Gazi University

Assoc. Prof. Dr. Umut Orguner _____
Electrical and Electronics Engineering Dept., METU

Assist. Prof. Dr. Ozan Keysan _____
Electrical and Electronics Engineering Dept., METU

Date: 12.07.2016

I hereby declare that all information in this document has been obtained and presented in accordance with academic rules and ethical conduct. I also declare that, as required by these rules and conduct, I have fully cited and referenced all material and results that are not original to this work.

Name, Last Name : AHMET ÖNER

Signature :

ABSTRACT

STATE ESTIMATION BASED FAULT LOCATION USING PMU MEASUREMENTS

Öner, Ahmet
M.Sc., Department of Electrical & Electronics Engineering
Supervisor : Assist. Prof. Dr. Murat Göl

July 2016, 60 Pages

Accurate location of a permanent fault on a transmission line is extremely important to restore the service in the shortest time possible, which directly affects the operational cost and system reliability. There are measurement based fault location methods in the literature, which require a high number of installed devices at substations. In this thesis study, an accurate and computationally fast strategy for fault location based on well-known Weighted Least Squares state estimator is presented.

The proposed method employs Phasor Measurement Unit (PMU) measurements recorded during the fault, due to the fast refresh rate of PMUs. PMUs provide synchronized voltage and current measurements. The synchronization of the PMU measurements is achieved using Global Positioning System (GPS). Those measurements are used to identify the faulted line via the estimated current flows in the system and then locate the fault on the flagged line disregarding the value of the fault impedance.

The proposed method makes use of multiple PMU measurements received in consecutive time instants and hence reduces the required number of measurements for the solution of the fault location problem. Moreover, use of those multiple measurements improves the robustness of the proposed method against the bad data and incorrect parameters.

The fault location problem is also solved with a modified formulation in order to show the robustness of the proposed method against the incorrect line parameters. The modified formulation includes estimation of the line parameters with multiple PMU measurements.

The proposed method has an iterative solution, because of the non-linearity between the measurements and the states to be determined. This thesis also shows the importance of the initial values and indicates comments on selection of those values.

The proposed method is validated using synthetic data in different computational environments.

Keywords: Fault Location, Least Squares Estimation, Phasor Measurement Units (PMU), State Estimation

ÖZ

FAZÖR ÖLÇÜM BİRİMİ ÖLÇÜMLERİ İLE DURUM KESTİRİMİ TEMELLİ HATA LOKALİZASYONU

Öner, Ahmet
Yüksek Lisans, Elektrik & Elektronik Mühendisliği Bölümü
Tez Yöneticisi : Yard. Doç. Dr. Murat Göl

Temmuz 2016, 60 Sayfa

Bir iletim hattı üzerindeki daimi hatanın en kısa sürede onarılabilmesi için hatanın doğru bir şekilde lokalize edilmesi önem arz etmektedir. Hatanın en kısa sürede onarılması işletme maliyetini ve sistem güvenilirliğini doğrudan etkilemektedir. Literatürde, trafo merkezlerine yüksek miktarda ölçüm cihazı kurulumu gerektiren ölçüm temelli hata lokalizasyonu methodları bulunmaktadır. Bu tez çalışmasında, Ağırlıklandırılmış En Küçük Kareler durum kestirimi methoduna dayalı hata lokalizasyonunun hassas ve hızlı hesaplanabilir bir yöntemi sunulmaktadır.

Önerilen method, Fazör Ölçüm Birimlerinin yüksek yenilenme hızı sayesinde, hata sırasında kaydettiği ölçümleri kullanmaktadır. Fazör Ölçüm Birimleri, senkronize voltaj ve akım ölçümleri sağlamaktadır. Fazör Ölçüm Birimi ölçümlerinin senkronizasyonu Küresel Konumlama Sistemi kullanılarak gerçekleştirilmektedir. Bu ölçümler, sistem üzerinde kestirimi yapılan akımlar üzerinden hatalı hattın belirlenmesinde kullanılmaktadır. Daha sonra, hatalı olarak işaretlenen hattın hata konumu, hata empedansı ihmal edilerek bulunmaktadır.

Önerilen method, Fazör Ölçüm Birimlerinin art arda ölçüm alabilmesinden faydalanmaktadır. Dolayısı ile hata lokalizasyonu probleminin çözümü için ihtiyaç duyulan ölçüm sayısını azaltmaktadır. Buna ek olarak, birden çok ölçümün kullanılması hatalı veriye ve yanlış parametrelere karşı gürbüzlük sağlamaktadır.

Önerilen methodun hatalı veri altında gürbüzlüğünü göstermek amacıyla hata lokalizasyonu problemi modifiye edilmiş formülasyon ile de çözülmüştür. Formülasyondaki değişiklik Fazör Ölçüm Birimlerinin art arda ölçüm alabilmesinden faydalanarak hat parametrelerinin kestirimini içermektedir.

Önerilen method, ölçümler ve hata konumları arasındaki doğrusal olmayan ilişki sebebiyle yinelemeli çözüme sahiptir. Bu tez, aynı zamanda başlangıç değerlerinin önemini göstermekte olup bu değerlerin seçim işlemini yorumlamaktadır.

Önerilen method, farklı ortamlardaki yapay veriler kullanılarak doğrulanmıştır.

Anahtar Kelimeler: Hata Lokalizasyonu, En Küçük Kareler Kestirimi, Fazör Ölçüm Birimleri, Durum Kestirimi

To My Family

ACKNOWLEDGMENTS

First of all, I would like to thank and express my deepest gratitude to my supervisor and mentor Murat Göl, for his support, guidance and encouragement. His guidance will shape my future.

I thank my parents for their endless trust and support throughout my life. I also would like to thank my brother, Alper, for his help and patience during my studies.

I am also grateful to ASELSAN Inc. for her opportunities and supports during the completion of this thesis.

TABLE OF CONTENTS

LIST OF TABLES

TABLES

LIST OF FIGURES

FIGURES

LIST OF ABBREVIATIONS

ANSI	: American National Standards Institute
BLUE	: Best Linear Unbiased Estimator
EMS	: Energy Management System
GPS	: Global Positioning System
IEEE	: Institute of Electrical and Electronics Engineers
LAV	: Least Absolute Value
MAE	: Mean Absolute Error
pMAE	: Percentage Mean Absolute Error
PMU	: Phasor Measurement Unit
SCADA	: Supervisory control and data acquisition
SE	: State Estimation
WLS	: Weighted Least Squares

CHAPTER 1

INTRODUCTION

In recent years, power systems in the world have rapidly grown due to the raise in the electricity demand, which resulted in complicated system structures with a very high number of transmission lines. Those lines are exposed to faults in different ways such as lightning strokes, storms and short circuits due to contacts of trees, which may cause permanent faults on the transmission lines. To be able to clear the permanent faults in the shortest time, and to improve the power quality, system security and the reliability of the grid, fault location is required. In the literature many fault location methods are presented [1] – [24].

The fault location methods can be divided into two categories. Among the methods presented in the literature, a good number of impedance-based fault location algorithms, which are performed at the power frequency, have been developed [1] – [16]. Those algorithms use bus voltage and line current data of either a single bus (one-ended) [2] – [5] or both buses (two-ended) [6] – [10] that are connected to the faulted line. Multi-bus algorithms, which use measurements taken from the ends of the multi-terminal transmission lines, are also available in the literature [11] – [16].

The second group of the fault location methods is based on high-frequency components of the fault-transient signals, which may be called traveling-wave based fault-location methods [17] – [24]. Those methods use the correlation between traveling waves, which propagate along the transmission lines. Although, those

methods are more accurate compared to impedance-based methods, they require special equipment designed to collect raw data with acceptable precision, which increases the cost of fault location significantly.

This thesis proposes use of two-terminal impedance-based fault location using Phasor Measurement Unit (PMU) data, which are populating in power systems since 2003. PMUs measure synchronized voltage and current phasor measurements with respect to the Global Positioning System (GPS), which provides access to an accurate global clock. They have a great advantage in managing the power system thanks to their fast refresh rates. Typically, PMUs refreshing rate is 30 scans per second [25] – [26].

The main motivation of the thesis is to identify faulted lines in a given system and locate the faults on the identified lines to enable service providers restore the service in the shortest time possible, which will increase the power quality and the reliability of the grid. In order to reduce the effects of the measurement errors, and incorrect system parameter information, which is quite possible due to varying weather conditions, this work employs state estimation methods to identify the faulted lines and locate the faults along the identified transmission lines.

For power quality, system security and sustainability, and reliability of the service, Energy Management System (EMS) is used to monitor, control and optimize the performance of the generation and transmission systems. Operators of EMS need reliable information for proper operation. Therefore, state estimation is one of the most important tools of the EMS. State estimators;

- Estimate bus voltages, branch flows, etc. (state variables),
- Provide measurement error processing results,
- Give an estimate for all metered and unmetered quantities,

- Filter out small errors due to model approximations and measurement inaccuracies,
- Detect and identify discordant measurements, called bad data.

This thesis proposes a state estimation based fault location method, which employs the well-known two-ended algorithm [6] – [10]. The method assumes that the considered system is PMU observable, such that the state estimation can be performed using only PMU measurements. Considering the increasing number of PMUs, it can be expected that this assumption will be realized in near future for many grids around the world. Use of PMUs enables use of measurements received at different time instants for fault location, which contributes the robustness to the state estimator. Moreover, thanks to the time synchronization in PMU observable systems, the fault location can be performed more accurately compared to the systems measured by conventional SCADA measurements.

The proposed method firstly performs power system state estimation [27] to determine the voltages of each bus, which may be called as EMS state estimator. Assuming the considered system's measurement design is redundant enough, such that bad data can be identified, the fundamental component of the faulted current flowing through the line from both sending and receiving ends can be calculated. Note that this part is especially necessary if sending end and/or receiving end of the faulted line is not measured by a PMU.

Once the faulted line is identified, Weighted Least Squares (WLS) estimator is employed to locate the fault on the identified transmission line. WLS uses estimates of the line currents and bus voltages as well as the measurements obtained from PMUs corresponding to different time instants for measurement redundancy.

This thesis assumes that the conventional circuit breakers interrupt the fault current at least in 4 cycles [28]. Therefore, 2 measurement scans from the PMUs and hence 2

estimation sets are available, which provide the observation redundancy to perform a proper estimation.

State estimation was used for fault location previously [29]. The method in [29] modifies the state vector, by adding new system states for the location of the fault each time a fault is detected. If there is more than one fault in the system on different lines, [29] may not be able to find the fault locations because of the decreased redundancy, which may lead to an unobservable system. However, the proposed algorithm can determine the fault location, independent of the number of faults, since a separate state vector is formed for each fault.

The observation vector built by the proposed method includes current and voltage phasor measurements collected in consecutive time instants, which provides the observation redundancy to perform a proper estimation of the fault location. Moreover, the estimation results obtained from the EMS state estimator may contribute the measurement redundancy. Therefore, the proposed method never experiences a redundancy problem. Moreover, thanks to the small size of the fault location problem, the computational burden of the proposed method will be very small. The fault locations are determined using WLS estimator, which is the Best Linear Unbiased Estimator (BLUE) [30], such that the estimates will be the most accurate if there is only Gaussian error associated with the measurements.

The main objectives of the thesis can be listed as follows:

- Developing a state estimation based method to identify the faulted lines in a given system
- Locating the fault on the identified line, using state estimation.

The thesis consists of five chapters. Chapter 1 presents the thesis motivation and the literature survey on fault location methods. Chapter 2 reviews the WLS state estimation method and summarizes the iterative solution of WLS state estimation method based on Gauss-Newton method. Chapter 3 introduces the proposed method

and explains how to identify faulted lines using estimated fault currents, and how to build the fault location problem based on SE. Chapter 4 evaluates the performance of proposed fault location based on SE technique which builds a separate state vector to estimate the location of each fault. Finally, Chapter 5 consists of a summary of the work and main conclusions drawn.

CHAPTER 2

BACKGROUND

After presenting the general introduction and fault location algorithm methods in Chapter 1, this chapter will introduce the technical background, which will conduce the reader understand the presented study. Firstly, problem statement will be explained. Then, mathematical explanation of Weighted Least Squares (WLS) method will be provided. Finally, Iterative Solution of WLS (Gauss-Newton Method) approach will be introduced.

2.1 Problem Statement

This thesis investigates the problem of locating a fault in a power system using PMU measurements. The methods proposed in the literature [1] – [16] are directly based on the data obtained from the measurement devices. This work proposes use of state estimation instead of measurements, in order to minimize the effects of measurement and system model inaccuracies, and to decrease the number of devices that should be installed in the system. Therefore, this work proposes performing power system state estimation to determine the line flows that will point the faulted line. Then, the estimated voltages and currents as well as the corresponding measurements are used to locate the fault on the flagged transmission line. The Weighted Least Squares (WLS) estimator is employed in this study because of its speed and ease of

implementation. Moreover, it is known that WLS is the best linear unbiased estimator (BEST) under Gaussian noise [30]. The Weighted Least Squares and Iterative Solution of WLS (Gauss-Newton Method) are reviewed in this chapter.

2.2 Weighted Least Squares (WLS)

The observation vector *z* consists of measurements taken from the field. Assuming *z* is a nonlinear function of the system states (i.e. bus voltage and phase angle), this relation can be expressed mathematically as follows for an *n*-bus power system with *m* measurements:

$$z = \begin{bmatrix} z_1 \\ z_2 \\ \vdots \\ z_m \end{bmatrix} = \begin{bmatrix} h_1(x_1,\ x_2, \dots, x_n) \\ h_2(x_1,\ x_2, \dots, x_n) \\ \vdots \\ h_m(x_1,\ x_2, \dots, x_n) \end{bmatrix} + \begin{bmatrix} e_1 \\ e_2 \\ \vdots \\ e_m \end{bmatrix} = h(x) + e \tag{2.1}$$

where,

The $m \times 1$ measurement vector *z* is defined as follows.

$$z^T = [z_1 \quad z_2 \quad \dots \quad z_m] \tag{2.2}$$

The vector *h* represents the mathematical relation between the measurements and the state vector *x*

$$h^T = [h_1(x_1, x_2, \dots, x_n) \quad h_2(x_1, x_2, \dots, x_n) \quad \dots \quad h_m(x_1, x_2, \dots, x_n)] \tag{2.3}$$

The $n \times 1$ state vector *x* is defined as follows.

$$x^T = [x_1 \quad x_2 \quad \dots \quad x_n] \tag{2.4}$$

The $m \times 1$ measurement error vector *e* is defined as follows

$$e^T = [e_1 \quad e_2 \quad \dots \quad e_m] \tag{2.5}$$

It is assumed that:

- $E[e] = 0$
- Measurement errors are independent, i.e., $E[e_i e_j] = 0$ where i≠j such that the covariance matrix is diagonal:

$$Cov(e) = E[ee^T] = R = diag\{\sigma_1^2, \quad \sigma_2^2, \quad \ldots, \quad \sigma_m^2\} \tag{2.6}$$

Based on those definitions, the WLS objective function is given as below.

$$J(x) = \sum_{i=1}^{m} \frac{(z_i - h_i(x))^2}{R_{ii}} = [z - h(x)]^T R^{-1} [z - h(x)] \tag{2.7}$$

The minimization condition of objective function is expressed below:

$$g(x) = \frac{\partial J(x)}{\partial x} = -H^T R^{-1}[z - h(x)] = 0 \tag{2.8}$$

where $H(x) = \partial h(x)/\partial x$.

2.3 Iterative Solution of WLS (Gauss-Newton Method)

In (2.8), expanding $g(x)$ into its Taylor series around the state vector x^k gives the following expression.

$$g(x) = g(x^k) + G(x^k)(x - x^k) + H.O.T. = 0 \tag{2.9}$$

Neglecting the higher order terms (H.O.T.) leads to an iterative solution:

$$x^{k+1} = x^k - G(x^k)^{-1} g(x^k) \tag{2.10}$$

where,

k is the iteration index,

x^k is the solution vector at iteration k

$G(x^k)$ is the gain matrix, which is sparse, positive definite and symmetric if the system is observable.

$$G(x^k) = \frac{\partial g(x^k)}{\partial x} = H^T(x^k)R^{-1}H(x^k) \tag{2.11}$$

$$g(x^k) = -H^T(x^k)R^{-1}(z - h(x^k)) \tag{2.12}$$

The equation for the state estimation calculation is given by the expression

$$G(x^k)\Delta x^{k+1} = H^T(x^k)R^{-1}(z - h(x^k)) \tag{2.13}$$

where $\Delta x^{k+1} = x^{k+1} - x^k$

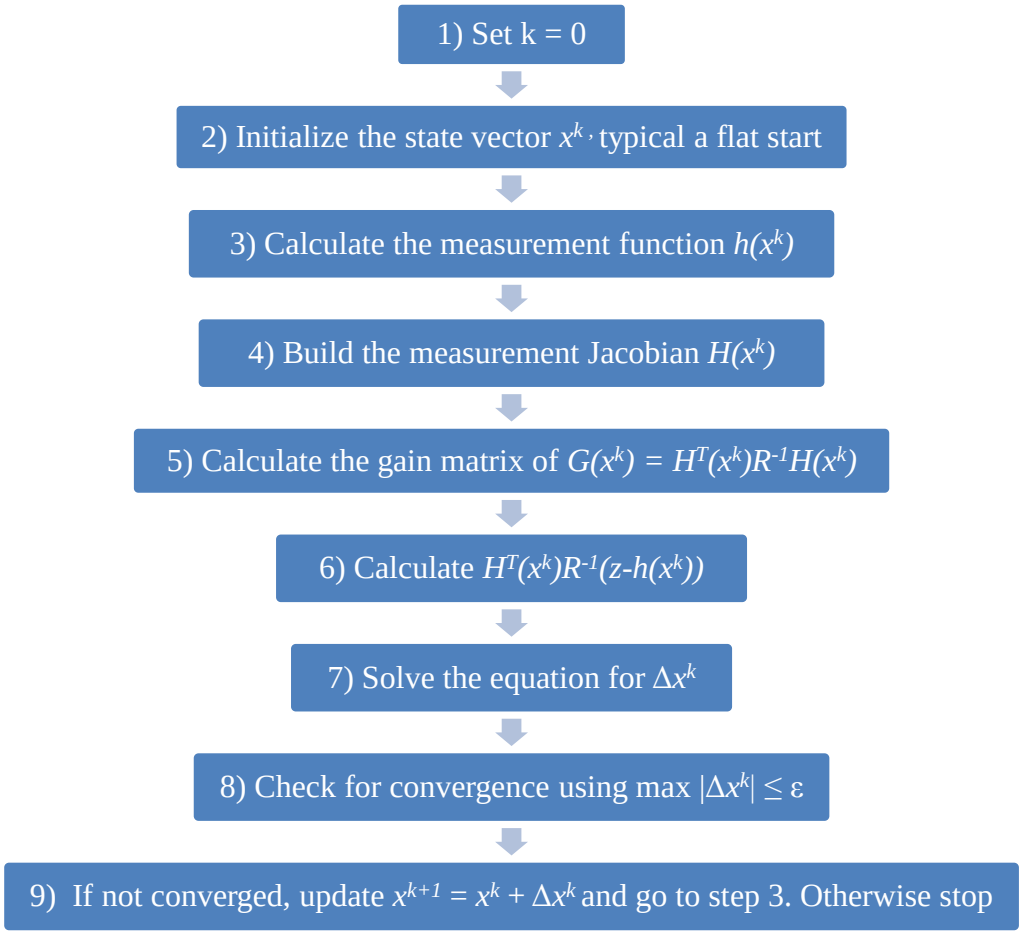

Figure 2-1 Summary of WLS State Estimation Algorithm

The WLS state estimation algorithm steps are summarized in Figure 2-1.

2.4 Normalized Residual Test

After the estimation process, state estimator may be deceived because of bad data. To detect the bad data, normalized residual test is performed.

In (2.14), linearized measurement model is given,

$$\Delta z = H\Delta x + e \tag{2.14}$$

where, Δz is measurement vector,

Δx is the true state vector,

H is Jacobian Matrix,

e is Gaussian error,

such that *E[e]=0* and *cov(e)=R.*

The WLS estimate can be found based on the linearized measurement model as follows.

$$\Delta\hat{x} = \underbrace{(H^T R^{-1} H)^{-1}}_{G^{-1}} H^T R^{-1} \Delta z \tag{2.15}$$

$$\Delta\hat{x} = G^{-1} H^T R^{-1} \Delta z \tag{2.16}$$

The estimated value of Δz is given in (2.17),

$$\Delta\hat{z} = H\Delta\hat{x} = K\Delta z \tag{2.17}$$

where $K = HG^{-1}H^TR^{-1}$

The properties of *K* matrix are given below:

- $K.K.K.K\ldots K = K$
- $K.H = H$

- *(I-K).H =0*

The measurement residuals can be computed as given in (2.18),

$$\begin{aligned} r &= \Delta z - \Delta \hat{z} \\ &= (I - K)\Delta z \\ &= (I - K)(H\Delta x + e) \\ &= (I - K)e \ \ (Since\ (I\text{-}K).H = 0) \\ &= Se \end{aligned} \tag{2.18}$$

where *S* is the residual sensitivity matrix.

The properties of *S* matrix are given below:

- *S.S.S.S…S = S*
- $S.R.S^T = S.R$

$$E(r) = E(S.e) = S.E(e) = 0 \tag{2.19}$$

$$\begin{aligned} Cov(r) = \Omega &= E[rr^T] \\ &= S.E[ee^T].S^T \\ &= SRS^T \\ &= SR \end{aligned} \tag{2.20}$$

Therefore, $r \sim N(0,\Omega)$ where Ω is residual covariance matrix.

$$r_i^N = \frac{|r_i|}{\sqrt{\Omega_{ii}}} = \frac{|r_i|}{\sqrt{R_{ii}S_{ii}}} \tag{2.21}$$

The normalized residual vector r^N will have a Standart Normal Distribution,

$r_i^N \sim N(0,1)$.

Therefore, a comparison between r^N and a statistical threshold can find the bad data if it exists. This threshold can be chosen based on the desired level of detection sensitivity.

CHAPTER 3

THE PROPOSED METHOD

Chapter 2 described the problem, locating a fault in a power system using PMU measurements, and also described the solution technique for the problem. As mentioned in Chapter 1, in order to solve the problem and determine the fault location, Weighted Least Squares (WLS) estimator is employed. In this chapter, the stages of the proposed method will be explained. Firstly, the method to determine the fault currents and hence identify the faulted line will be explained. Then, the fault location based on state estimation on the identified transmission line will be explained in detail.

3.1 State Estimation Based Identification of Faulted Lines

Identification of the faulted line is conducted based on the circuit breaker status in a well-monitored power system. This work proposes use of fault current estimates to determine the faulted line in the interconnected system using well-known WLS estimator. Note that for a proper operation of an Energy Management System a properly running state estimator is required. The proper state estimator consists of observability analysis, state estimation, which is assumed to be WLS in this work, and bad data analysis [27]. The proposed method makes use of state estimation and bad data analysis tools of EMS.

To be able to run the state estimator and hence compute the line currents, transmission system model, i.e. system connectivity and parameters (branch resistance, branch reactance, shunt conductance, shunt susceptance) are necessary. Moreover, the system should be observable, such that there should be a unique solution of the state estimation problem. This thesis assumes that the considered systems are PMU observable, such that the state estimation can be performed using only PMU measurements. Note that considering the rapid increase of the synchropahor measurements in the transmission grids, this assumption will be applicable in the near future for many transmission grids around the world. Minimum number of PMUs and installation locations can be found using [31].

PMU measurements are linearly related to the system states, which are bus voltage phasors, on the contrary of the conventional power flow measurements. Therefore the relation between the PMU measurements and the system states can be defined as below:

$$z^{PMU} = H^{PMU} x^{PMU} + e \tag{3.1}$$

where

$$x^{PMU} = \begin{bmatrix} Re\,\{V_i\} \\ Im\,\{V_i\} \end{bmatrix} \tag{3.2}$$

$$H^{PMU} = \begin{bmatrix} \frac{\partial V_i^{m,r}}{\partial V_i^r} & \frac{\partial V_i^{m,r}}{\partial V_j^r} & \frac{\partial V_i^{m,r}}{\partial V_i^i} & \frac{\partial V_i^{m,r}}{\partial V_j^i} \\ \frac{\partial V_i^{m,i}}{\partial V_i^r} & \frac{\partial V_i^{m,i}}{\partial V_j^r} & \frac{\partial V_i^{m,i}}{\partial V_i^i} & \frac{\partial V_i^{m,i}}{\partial V_j^i} \\ \frac{\partial I_{ij}^{m,r}}{\partial V_i^r} & \frac{\partial I_{ij}^{m,r}}{\partial V_j^r} & \frac{\partial I_{ij}^{m,r}}{\partial V_i^i} & \frac{\partial I_{ij}^{m,r}}{\partial V_j^i} \\ \frac{\partial I_{ij}^{m,i}}{\partial V_i^r} & \frac{\partial I_{ij}^{m,i}}{\partial V_j^r} & \frac{\partial I_{ij}^{m,i}}{\partial V_i^i} & \frac{\partial I_{ij}^{m,i}}{\partial V_j^i} \end{bmatrix} \tag{3.3}$$

In (3.3),

- H^{PMU} is constant Jacobian matrix (with dimension 4m x 2n) for PMU only systems where m is the number of measurement (for observable system) and n is the number of buses of the power system.
- V is the solution vector where V_i and V_j are the solution voltages of 2 buses.

Note that, in (3.3), H^{PMU} is given for 2-Bus system.

Instead of computing each entry of (3.3), the relation between the bus voltages and line current can be used to build H^{PMU}, which is defined as follows.

$$I_{ij}^{m,r} = g_{ij}\left(V_i^r - V_j^r\right) - b_{ij}\left(V_i^i - V_j^i\right) - b_{ii}V_i^i + e \tag{3.4}$$

$$I_{ij}^{m,i} = g_{ij}\left(V_i^i - V_j^i\right) - b_{ij}\left(V_i^r - V_j^r\right) - b_{ii}V_i^r + e \tag{3.5}$$

In (3.4) and (3.5),

- g_{ij} is the shunt conductance between Bus-i and Bus-j,
- b_{ij} is the shunt susceptance between Bus-i and Bus-j,
- b_{ii} is the half of the total line charging for Bus-i,
- V_i^i is the imaginary part of the system state voltage of Bus-i,
- V_i^r is the real part of the system state voltage of Bus-i,
- V_j^i is the imaginary part of the system state voltage of Bus-j,
- V_j^r is the real part of the system state voltage of Bus-j,
- e is the measurement error,
- $I_{ij}^{m,r}$ is the real part of the measured current between Bus-i and Bus-j,
- $I_{ij}^{m,i}$ is the imaginary part of the measured current between Bus-i and Bus-j.

Considering (3.3), (3.4) and (3.5), it can be said that H^{PMU} has the following general structure, where the first two rows correspond to real and imaginary parts of voltage phasor measurements, respectively, and last two rows correspond to real and imaginary parts of the current phasor measurements, respectively.

$$H^{PMU} = \begin{bmatrix} 1 & 0 & 0 & 0 \\ 0 & 0 & 1 & 0 \\ g_{ij} & -g_{ij} & -b_{ij} - b_{ii} & b_{ij} \\ b_{ij} + b_{ii} & -b_{ij} & g_{ij} & -g_{ij} \end{bmatrix} \tag{3.6}$$

From (3.6), (3.7) and (3.8), state estimation problem can be solved as follows.

$$(H^{PMU})^T R^{-1} z^{PMU} = \underbrace{(H^{PMU})^T R^{-1} H^{PMU}}_{G^{PMU}} \hat{x} \tag{3.7}$$

$$G^{PMU} \hat{x} = (H^{PMU})^T R^{-1} z^{PMU} \tag{3.8}$$

where

- $\hat{x}$ (vector with dimension 2n x 1), is estimated state vector. n is the number of buses.
- R^{-1} (matrix with dimension 4m x 4m) is the measurement covariance matrix. m is the number of measurement.
- G^{PMU} (matrix with dimension 2n x 2n) is the gain matrix.
- z^{PMU} (vector with dimension 4m x 1) is the phasor measurement.

In the presence of a redundant enough measurement design for state estimation robustness [31], even if the SCADA fails the topology update, the faulted line can be identified. After the state estimation, the bad data process, namely normalized residuals test [32], will flag the current phasor measurements associated with the faulted line as bad measurements, because of the model mismatch due to the fault. Even if the EMS does not update the system topology, this strategy will show the

faulted line to the system operator. The summary of state estimation based identification of faulted lines is given in the Figure 3-1. Due to the model mismatch, the measurements associated with the faulted line will be flagged as bad measurements. Note that this method relies on the assumption that there is a redundant enough measurement set.

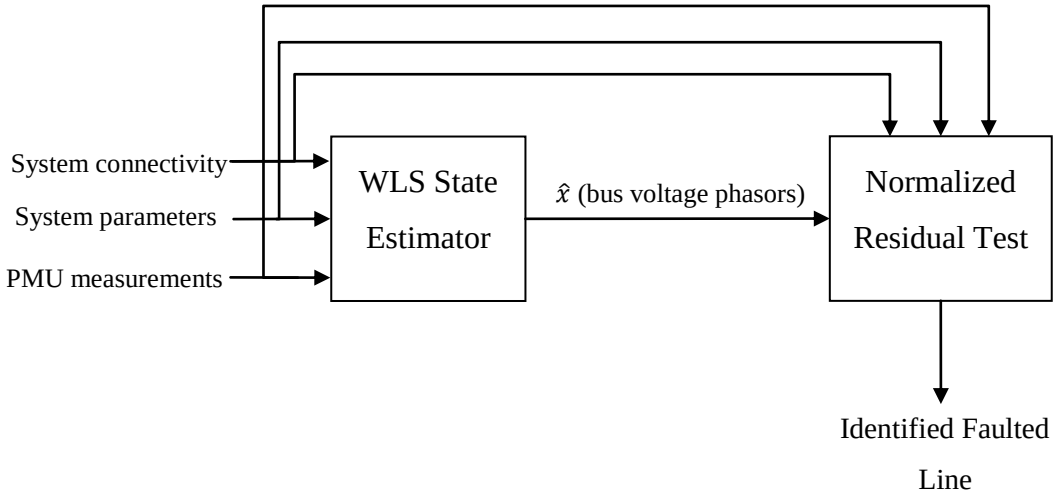

Figure 3-1 Summary of State Estimation Based Identification of Faulted Lines

The proposed method employs the two-ended fault location methods to locate the fault on the flagged line. Those methods require current measurements taken at the both ends of the faulted line. If a PMU does not exist at the sending end and/or receiving end, results of state estimation can be used to compensate the lack of that current measurement. In this work, the proposed method employs all the available PMU measurements associated with the faulted line as well as the voltage and current estimates obtained via the state estimator of the EMS to improve the measurement redundancy. Note that, use of current estimates for the fault location is

possible if there is no power injection at the bus without PMU or the amount of injected power is known.

Once the injection power is known, the fault current, I_f in Figure 3-2 can be calculated as follows, using the famous Kirchhoff's Current Law.

$$I_f = \sum_{k \in N} I_k \tag{3.9}$$

In (3.9), N represents the set of lines connected to Bus-1. Note that, once the fault occurs the system model corresponding to the faulted line will not be correct any more. Therefore, the fault current cannot be calculated using the voltage estimates of the sending and receiving end buses, but rather (3.9) should be employed.

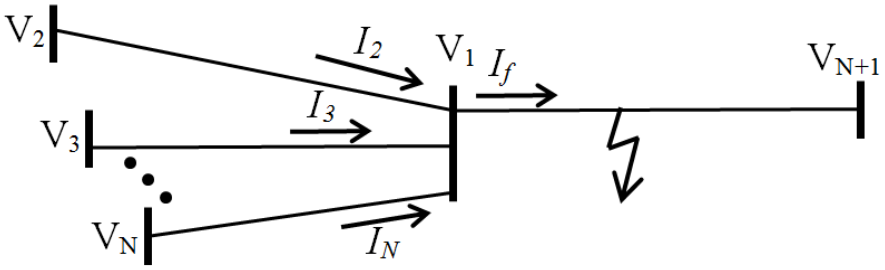

Figure 3-2 Calculation of fault current using state estimates

3.2 Fault Location on a Transmission Line Based on State Estimation

The synchronized two-ended method solves the following two equations simultaneously in order to locate the fault shown in Figure 3-3. In (3.10) and (3.11), the transmission line is modelled as nominal Π. In nominal Π model, the total lumped shunt admittance is divided into two equal halves, and each half with value b_{ii} and b_{jj} is placed at both the sending and the receiving end. In (3.10), I_{fi} is the

current flowing through sending end of the circuit. In other words, the total current of I_{fi} is the sum of currents flowing through the admittances and currents flowing through the impedance between the fault and sending end bus (Zα). In (3.11), I_{fj} is the current flowing through receiving end of the circuit. The total current of I_{fj} is the sum of the current flowing to the ground through the shunt admittance and the current flowing through the impedance between the fault and receiving end bus (Z(1-α)).

$$I_{fi} = \frac{V_i - V_f}{\alpha Z} + V_i b_{ii} \alpha \tag{3.10}$$

$$I_{fj} = \frac{V_j - V_f}{(1-\alpha) Z} + V_j b_{jj} (1-\alpha) \tag{3.11}$$

where V_i, V_j and V_f are the voltage phasors at Bus-i, Bus-j and the fault location, respectively. Fault current flowing through Bus-*i* is represented by I_{fi}, while fault current flowing through Bus-*j* is represented by I_{fj}. *Z* represents the series impedance of the line between buses *i* and *j*, and b_{ii} and b_{jj} represent the line charging susceptances at Bus-*i* and Bus-*j*, respectively. Finally, α shows the ratio of the distance of the fault to Bus-*i* to the total length of the faulted line.

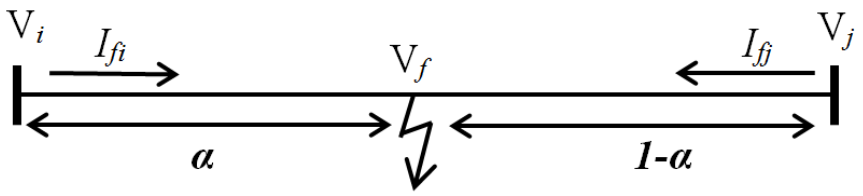

Figure 3-3 Sample faulted line

Conventional two-ended synchronized fault location solves (3.10) and (3.11) to find α and V_f by disregarding the value of the fault impedance. It is known that PMU data carry measurement error, which is assumed Gaussian. Moreover, due to the transient

during the clearance of the fault, calculated phasors may be erroneous. This work proposes use of WLS estimator to calculate the fault location (α) in order to minimize the effects of measurement errors.

Successful error removal requires measurement redundancy [31]. Therefore, proposed method uses all measurements and state estimates, if required, recorded from the beginning of the fault until the clearance of the fault. Considering the opening time of a circuit breaker, the proposed method can use at least two PMU scans for fault location as shown in Figure 3-4. Note that, Figure 3-4 is generated for visualization purposes and it is not a result of simulation tool. If PMUs are re-programmed to scan 60 times a second during a fault, instead of conventional refreshing rate of 30 scans per second, the number of observations will be increased to four and hence a more reliable estimation will be possible.

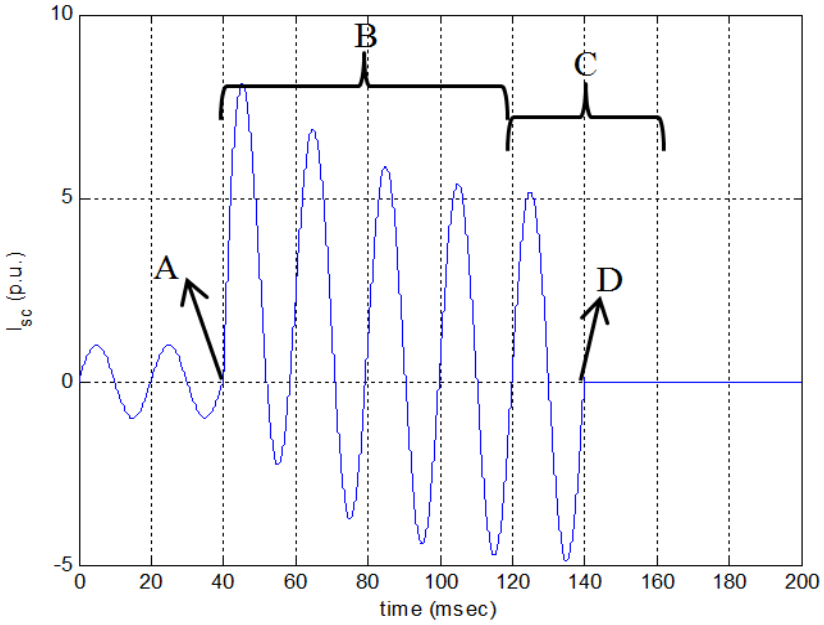

Figure 3-4 Sample fault current time variation

In Figure 3-4, "A" indicates the beginning time of the fault, and "B" shows the duration that PMU measurements can be used, assuming that PMU refresh rate is 30 scans per second. During "B" two sets of voltage and current phasor measurements

will be received. The data recorded during "C" cannot be used, since some of it includes data taken after the opening of the circuit breaker, which corresponds to the point "D". This work employs the measurements during "B" for fault location.

WLS estimator is employed to solve the non-linear estimation problem, where (3.10) and (3.11) are the relations between the state vector and observation vector. The state vector, *x*, is defined as follows.

$$x^T = \begin{bmatrix} V_f^{r,m} & V_f^{i,m} & \alpha_1 & \alpha_2 \end{bmatrix} \tag{3.12}$$

In (3.12);

$\alpha_1 = \alpha$, and $\alpha_2 = 1 - \alpha$,

$V_f^{r,m}$ is the real part of the voltage phasor at the fault location at time instant-m,

$V_f^{i,m}$ is the imaginary part of the voltage phasor at the fault location at time instant-m.

For two measurement scans from the PMUs, the state vector is as follows.

$$x^T = \begin{bmatrix} V_f^{r,1} & V_f^{r,2} & V_f^{i,1} & V_f^{i,2} & \alpha_1 & \alpha_2 \end{bmatrix} \tag{3.13}$$

In the proposed problem formulation observation vector consists of fault current measurements and estimates, if necessary, taken at consecutive time instants.

$$z^T = \begin{bmatrix} I_s^{r,1} & I_r^{r,1} & I_s^{r,2} & I_r^{r,2} & I_s^{i,1} & I_r^{i,1} & I_s^{i,2} & I_r^{i,2} \end{bmatrix} \tag{3.14}$$

where

- $I_s^{r,1}$ is the real part of the measured current of sending end of the faulted line at first time instant,
- $I_r^{r,1}$ is the real part of the measured current of receiving end of the faulted line at first time instant,

- $I_s^{r,2}$ is the real part of the measured current of sending end of the faulted line at second time instant,
- $I_r^{r,2}$ is the real part of the measured current of receiving end of the faulted line at second time instant,
- $I_s^{i,1}$ is the imaginary part of the measured current of sending end of the faulted line at first time instant,
- $I_r^{i,1}$ is the imaginary part of the measured current of receiving end of the faulted line at first time instant,
- $I_s^{i,2}$ is the imaginary part of the measured current of sending end of the faulted line at second time instant,
- $I_r^{i,2}$ is the imaginary part of the measured current of receiving end of the faulted line at second time instant.

At the consecutive time instants, the observation vector (3.14) of faulted line can be obtained from PMU. If a PMU does not exist at the sending end and/or receiving end of the faulted line, results of state estimation can be used to compensate the lack of that voltage and current measurement.

The estimation problem is non-linear as mentioned previously, which indicates multiple mathematical solutions for the problem but only one feasible solution. Because of the non-linearity, the estimation problem is solved iteratively, starting from an initial condition. In fault location estimation the initial value of α, which is represented as $\alpha_{0,}$ has a major importance, since inappropriate values may lead to the unfeasible solution which is far from reality. Experiments showed that if one of the following conditions is satisfied, the estimation problem might converge to the unfeasible solution.

$$\alpha_0 \cong 1 - \alpha \tag{3.15}$$

$$\alpha_0 \cong \alpha \tag{3.16}$$

In this work, it is proposed to use small α_0, i.e. 0.01 to analyze unfeasible solutions. Note that, if unfeasible solution is found, the fault will be at a very close distance to the receiving or sending end bus.

It is observed that if the initial condition, α_0, is selected small (very close to 0) then the fault will be at sending end bus. If the initial condition, α_0, is selected big (very close to 1) then the fault will be at receiving end bus.

CHAPTER 4

SIMULATION RESULTS

In Chapter 3, determination of fault currents and fault location on a transmission line based on state estimation were proposed, after the introduction of technical background in Chapter 2. In this chapter, the fault location performance of the state estimation based method is investigated.

The simulations are performed using IEEE 14 Bus Test Case of the American Electric Power System (in the Midwestern US) and its parameters. Visualization of IEEE 14 Bus Test Case System and the PMU locations can be seen in Figure 4-1. IEEE 14 Bus Test Case System bus data are given in Table 4-1 and branch data are given in Table 4-2.

The PMU measurements are placed according to the method presented in [31] to satisfy the estimation robustness against bad data. The simulations include noise in voltage and current measurements. The noise is assumed to have Gaussian distribution. Standard deviation of the voltage phasor measurement is 0.001 pu and that of current phasor measurement is 0.004 pu. Measurements are obtained by adding Gaussian error to the power flow solution of the IEEE 14 Bus Test Case.

In Section 4.1, the proposed faulted line identification is verified. In Section 4.2, the proposed fault location method is verified. In Section 4.3, the effect of incorrect line parameters on fault location is investigated. In Section 4.4, multiple fault

identification using the proposed method is examined. Finally, in Section 4.5, the simulation results are discussed.

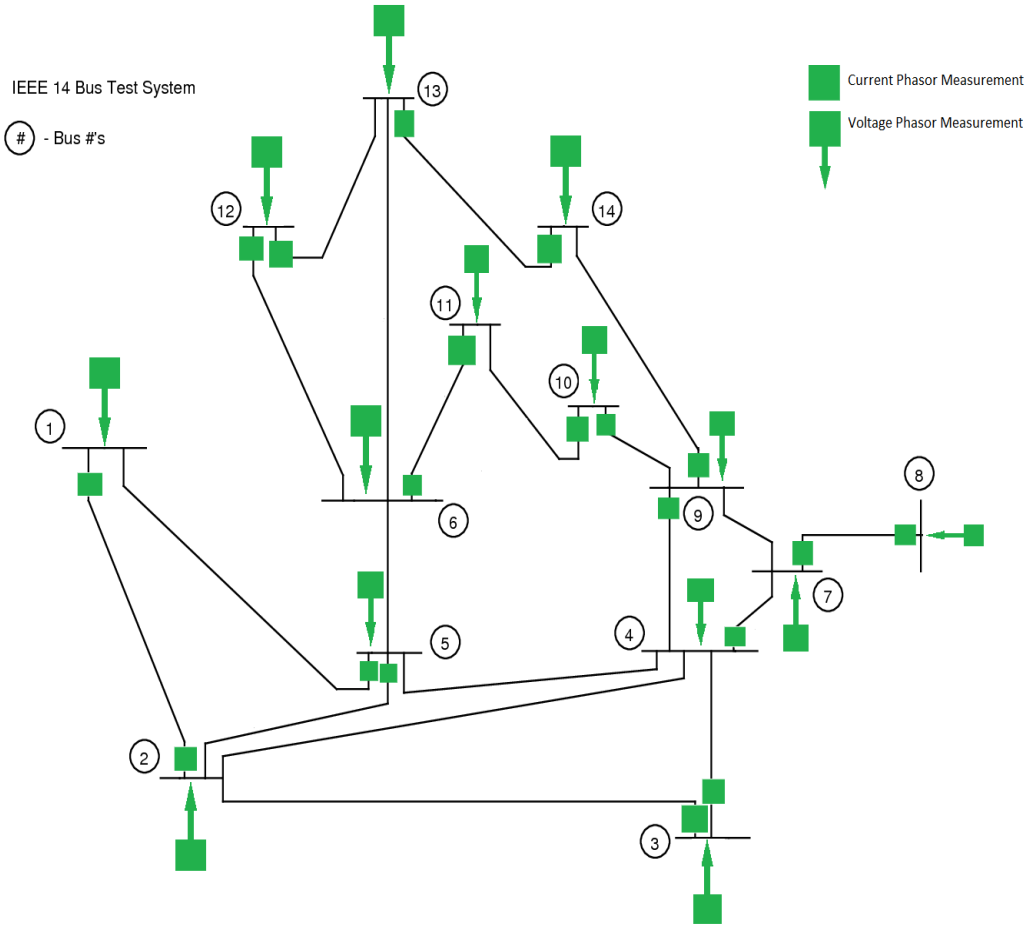

Figure 4-1 IEEE 14 Bus Test Case System

Table 4-1 Bus Data of IEEE 14 Bus Test Case System

Bus	**Load [MW]**	**Load [MVAR]**	**Generation [MW]**	**Generation [MVAR]**	**Shunt Susceptance B (per unit)**
1	0	0	232.4	-.16.9	0
2	21.7	12.7	40	42.4	0
3	94.2	19	0	23.4	0
4	47.8	-3.9	0	0	0
5	7.6	1.6	0	0	0
6	11.2	7.5	0	12.2	0
7	0	0	0	0	0
8	0	0	0	17.4	0
9	29.5	16.6	0	0	0.19
10	9	5.8	0	0	0
11	3.5	1.8	0	0	0
12	6.1	1.6	0	0	0
13	13.5	5.8	0	0	0
14	14.9	5	0	0	0

Table 4-2 Branch Data of IEEE 14 Bus Test Case System

From Bus	To Bus	Branch Resistance, R (per unit)	Branch Reactance, X (per unit)	Line Charging, B (per unit)	Transformer Tap Ratio
1	2	0.01938	0.05917	0.0528	0
1	5	0.05403	0.22304	0.0492	0
2	3	0.04699	0.19797	0.0438	0
2	4	0.05811	0.17632	0.034	0
2	5	0.05695	0.17388	0.0346	0
3	4	0.06701	0.17103	0.0128	0
4	5	0.01335	0.04211	0	0
4	7	0	0.20912	0	0.978
4	9	0	0.55618	0	0.969
5	6	0	0.25202	0	0.932
6	11	0.09498	0.1989	0	0
6	12	0.12291	0.25581	0	0
6	13	0.06615	0.13027	0	0
7	8	0	0.17615	0	0
7	9	0	0.11001	0	0
9	10	0.03181	0.0845	0	0
9	14	0.12711	0.27038	0	0
10	11	0.08205	0.19207	0	0
12	13	0.22092	0.19988	0	0
13	14	0.17093	0.34802	0	0

4.1 Verification of the Proposed Faulted Line Identification Method

This section aims to validate the proposed state estimation based faulted line identification. For this purpose, first, state estimation for EMS use is performed. Then, the bad data process, namely the largest normalized residuals test, is performed and based on the test results, the lines associated with the identified bad measurements are flagged as faulted lines. Note that, because of the model mismatch due to the fault, the related current flow measurements will be identified as bad measurements. Finally, iterative state estimation is performed to find fault location on the identified line.

The number of Monte Carlo runs is 500 to validate the proposed state estimation based faulted line identification. In each run, a three-phase to ground fault is located to a random line, based on a pre-determined α and a given α_0. The considered α and α_0 values are given in Table 4-3. The percentage Mean Absolute Error (pMAE) for each group of α and α_0 is calculated and presented in Table 4-3. Below is the formulation of pMAE where N is the simulation run number.

$$pMAE = 100 \times \frac{1}{N} \sum_{i=1}^{N} \left| \alpha_i^{estimated} - \alpha_i^{true} \right| \tag{4.1}$$

Note that the "unfeasible" solution encountered in Table 4-3 satisfies the condition (3.15), which means that using the given initial condition the feasible fault location estimation cannot be reached. This problem can be overcome by resolving the estimation problem with a different initial condition, α_0. Considering that the estimation problem solution is very fast, thanks to its small size, it can be concluded that this extra re-estimation step will not affect the computational performance significantly.

Table 4-3 pMAE for Different Fault Locations at Different Lines

pMAE		***α***		
		0.05	**0.5**	**0.95**
α₀	**0.005**	0.005 %	0 %	0 %
	0.01	0.0034 %	0 %	0 %
	0.02	0.0012 %	0%	0.0289 %
	0.05	0 %	0 %	unfeasible
	0.99	0 %	0 %	0.0033 %
	0.995	0 %	0 %	0.005 %

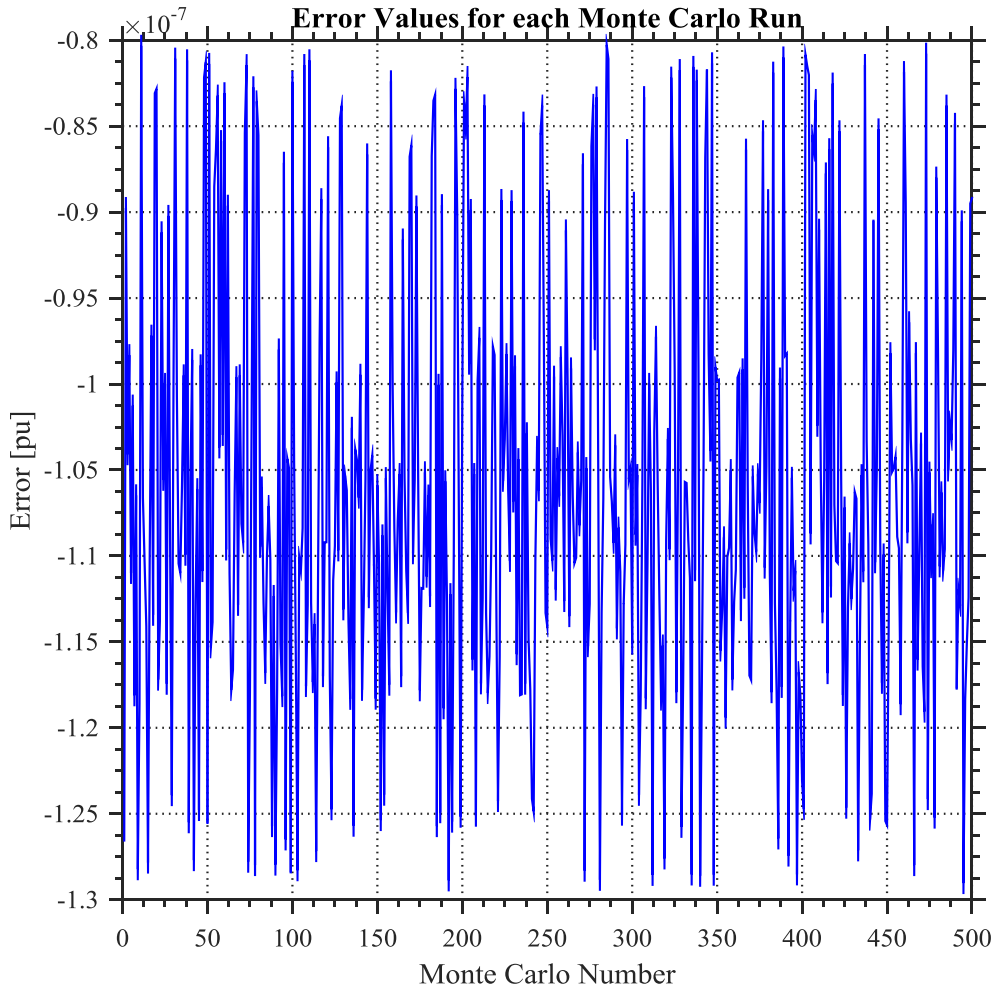

Figure 4-2 Error Between Estimated Location and Real Location for Different Lines (α_0: 0.005, α: 0.5)

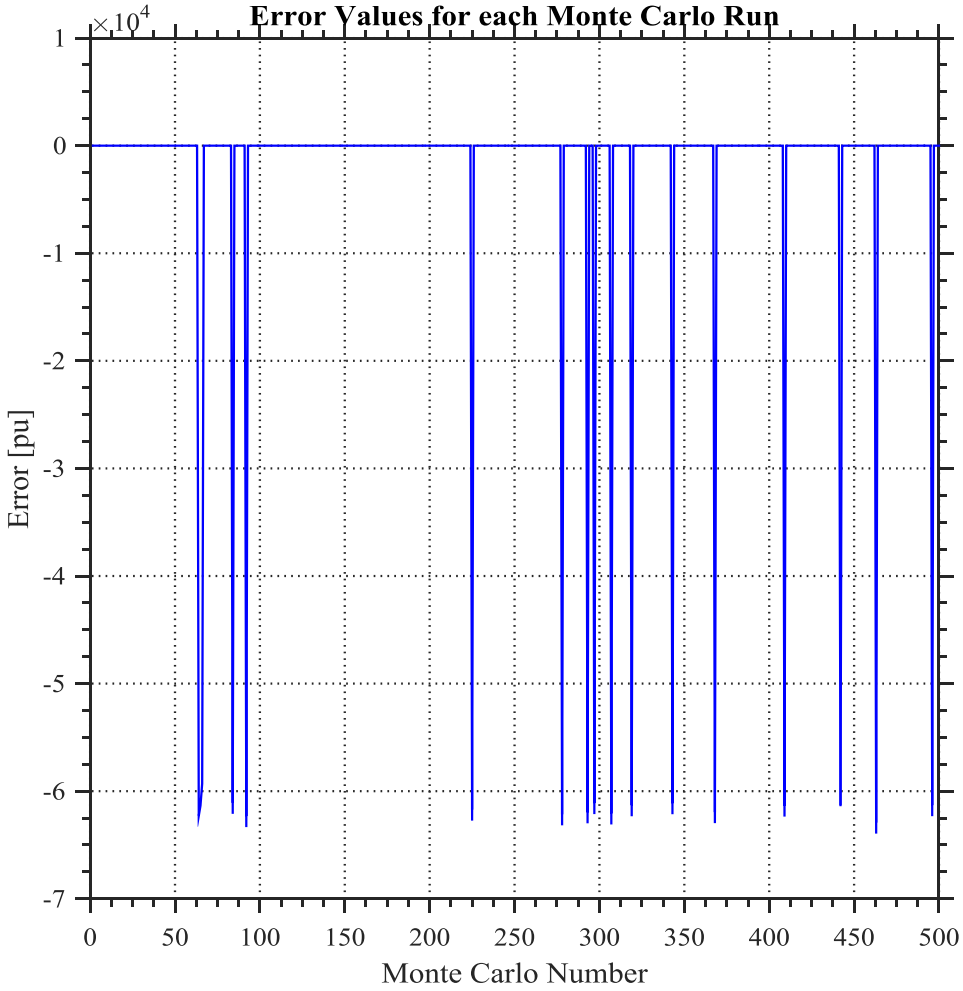

Figure 4-3 Error Between Estimated Location and Real Location for Different Lines (α_0: 0.05, α: 0.95)

Once the simulation results are investigated, it is found that all the faulted lines are identified correctly. However, the location of the fault on the identified line is not estimated correctly for some simulations. Figure 4-2 depicts that estimated location and real location is similar for all Monte Carlo results for the defined simulation case. On the other hand, Figure 4-3 depicts that the error between estimated location and real location has discrepancy for some of Monte Carlo results. This discrepancy

is caused by unfeasible solution, since (3.15) is satisfied. As explained previously, this issue can be solved with an extra re-estimation step.

In addition to the simulations explained so far, the proposed method is also tested with some realistic synthetic data obtained via DigSilent. A pre-determined line, namely the branch between Bus-1 and Bus-2, is assumed as faulted. In DigSilent, ANSI based short circuit (three-phase to ground) analysis is performed for the IEEE-14 bus system. In Figure 4-4, a sample screenshot of IEEE-14 bus system in DigSilent can be seen.

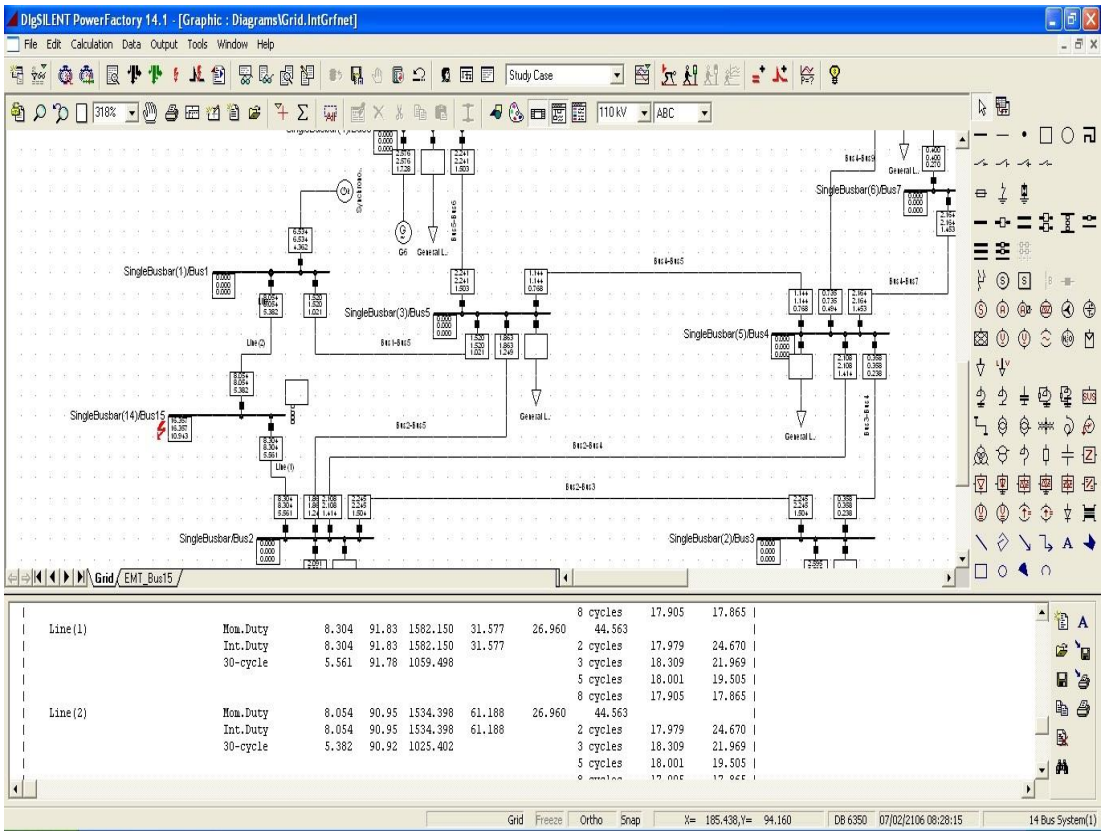

Figure 4-4 A Sample Screenshot of DigSilent while Short Circuit Analysis

Table 4-4 DigSilent Short Circuit Simulation Results for Different α Values

		I_{1f}		I_{2f}	
		Magnitude [A]	**Phase [degree]**	**Magnitude [A]**	**Phase [degree]**
α	**0.1**	9143	90.65	7220	92.33
	0.5	8054	90.95	8304	91.83
	0.7	7511	91.13	8849	91.62

DigSilent Short Circuit simulation results can be observed in Table 4-4.

Using the data in Table 4-4, the algorithm is run 100 times for each pre-determined α (0.1, 0.5 and 0.7) and a given α_0 (0.005). The percentage Mean Absolute Error (pMAE) for each α is calculated and presented in Table 4-5.

Table 4-5 pMAE for a Given Fault Locations using DigSilent Data

α_0 **= 0.005**		**pMAE**
α	**0.1**	0.072 %
	0.5	0.063 %
	0.7	0.056 %

Figure 4-5 shows the error between the estimated location and the real location, and depicts that this error is negligible for all selected α values.

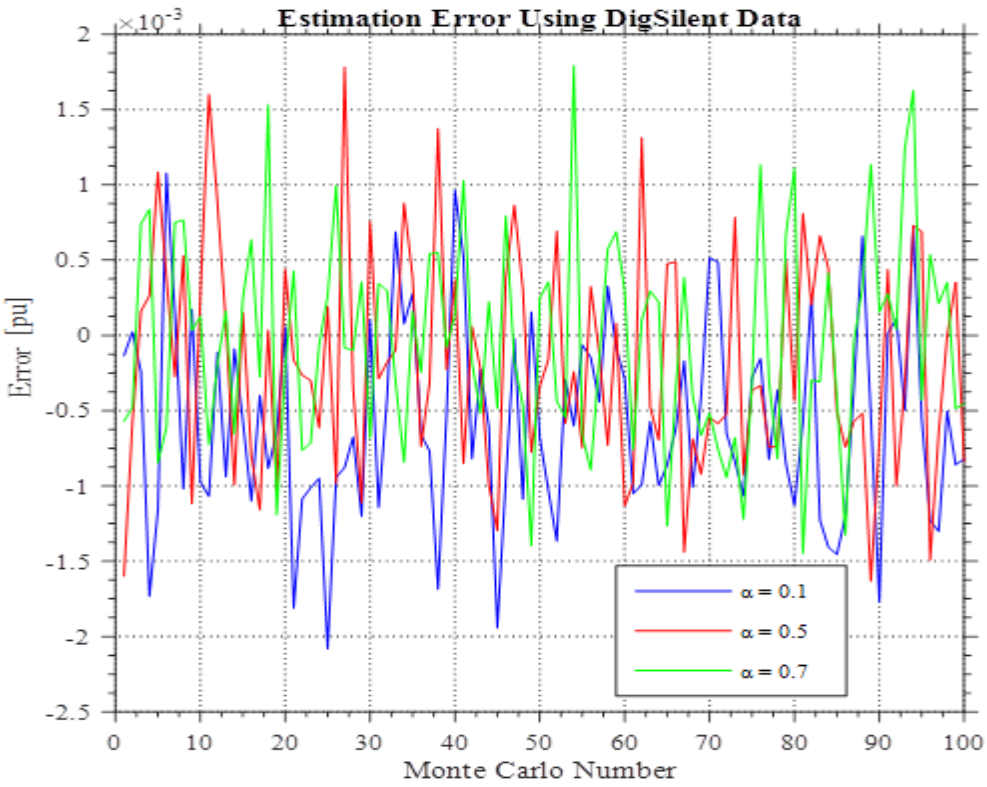

Figure 4-5 Performance of the Algorithm with DigSilent Data for Fault Between Bus-1 and Bus-2

The same approach is also conducted for the line between Bus-7 and Bus-8. The simulation results can be observed in Table 4-6.

Table 4-6 DigSilent Short Circuit Simulation Results for Different α Values

		I_{1f}		I_{2f}	
		Magnitude [A]	**Phase [degree]**	**Magnitude [A]**	**Phase [degree]**
α	**0.1**	9143	90.65	7220	92.33
	0.5	8054	90.95	8304	91.83
	0.7	7511	91.13	8849	91.62

The percentage Mean Absolute Error (pMAE) for each α is calculated and presented in Table 4-7.

Table 4-7 pMAE for a Given Fault Locations using DigSilent Data

α_0 = **0.005**		**pMAE**
α	**0.1**	0.0183 %
	0.5	0.0181 %
	0.7	0.0186 %

The performance of the algorithm with DigSilent data for fault between Bus-7 and Bus-8 can be seen in Figure 4-6. Figure 4-6 depicts that the error between estimated location and real location is negligible for all selected α.

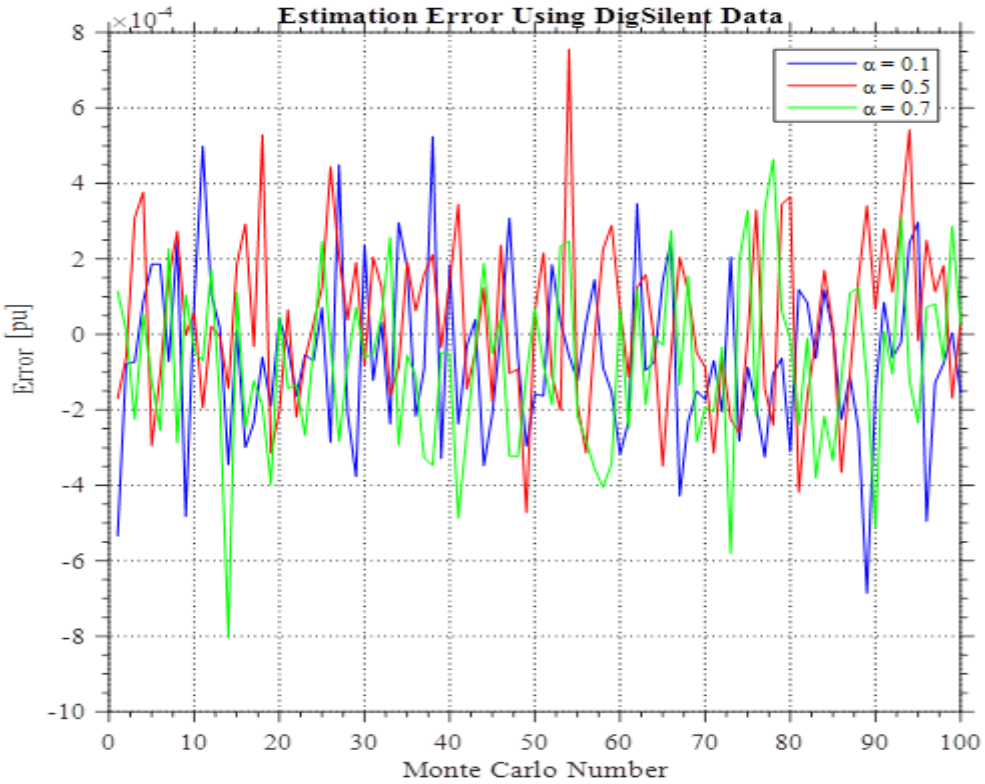

Figure 4-6 Performance of the Algorithm with DigSilent Data for Fault Between Bus-7 and Bus-8

4.2 Verification of the Proposed Fault Location Method

In this simulation, a pre-determined line, namely the one between the Bus-1 and Bus-2, is selected as the faulted line (three-phase to ground fault). Then Monte-Carlo simulations are run changing α randomly. This study is repeated 500 times for each α_0, which are defined in Table 4-8. The pMAE of the estimation values of α in all runs for different initial conditions are presented in Table 4-8. As seen in Table 4-8, the proposed method successfully locates the fault at a given line.

Table 4-8 pMAE for Different Fault Location at a Given Line

α_0	**pMAE**
0.005	0.1515 %
0.01	0.0355 %
0.02	0.0270 %
0.05	0.0242 %
0.99	0.0258 %
0.995	0.1589 %

Note that pMAE in Table 4-8 is calculated with respect to converged solutions. Diverged solutions are disregarded, assuming that they can be corrected by changing the initial condition. Errors for different fault location at a given line for each α_0 can be observed from Figure 4-7 through Figure 4-12.

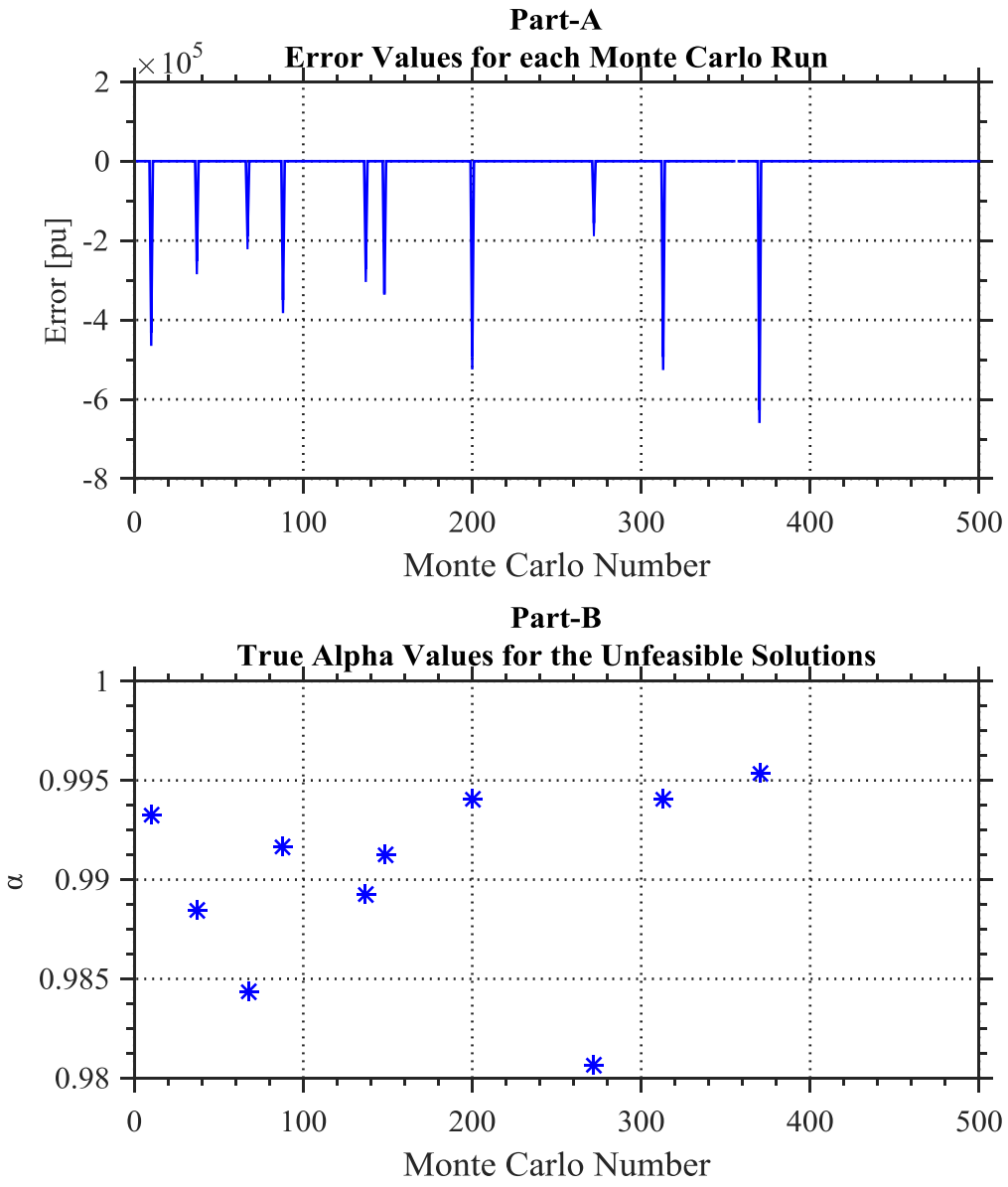

Figure 4-7 Error Between Estimated Location and Real Location for $\alpha_0 = 0.005$

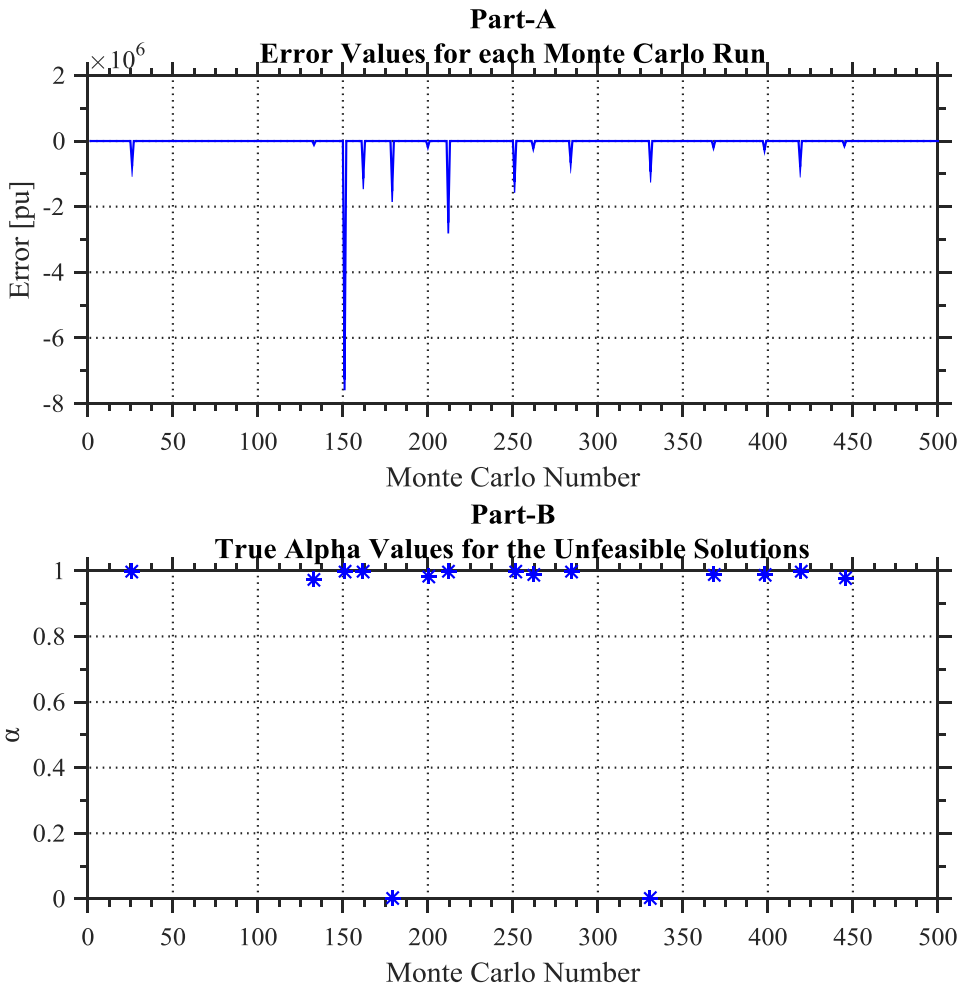

Figure 4-8 Error Between Estimated Location and Real Location for $\alpha_0 = 0.01$

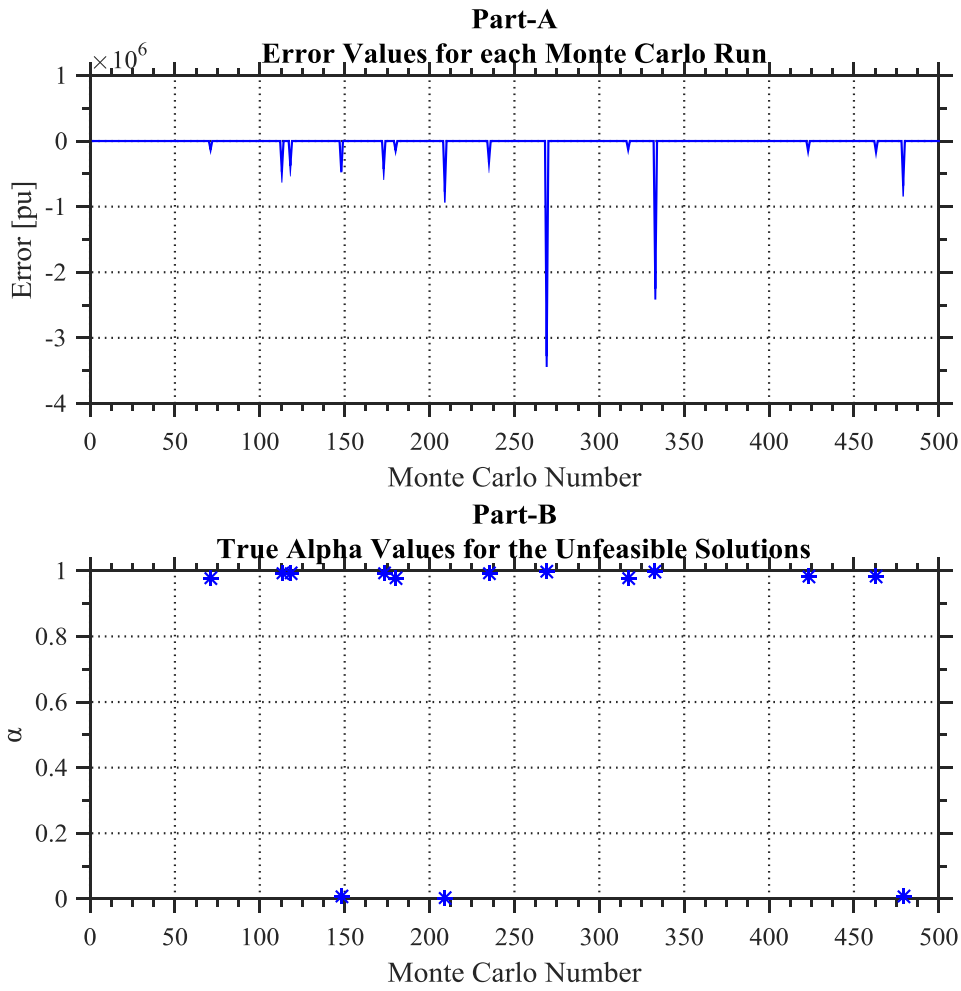

Figure 4-9 Error Between Estimated Location and Real Location for $\alpha_0 = 0.02$

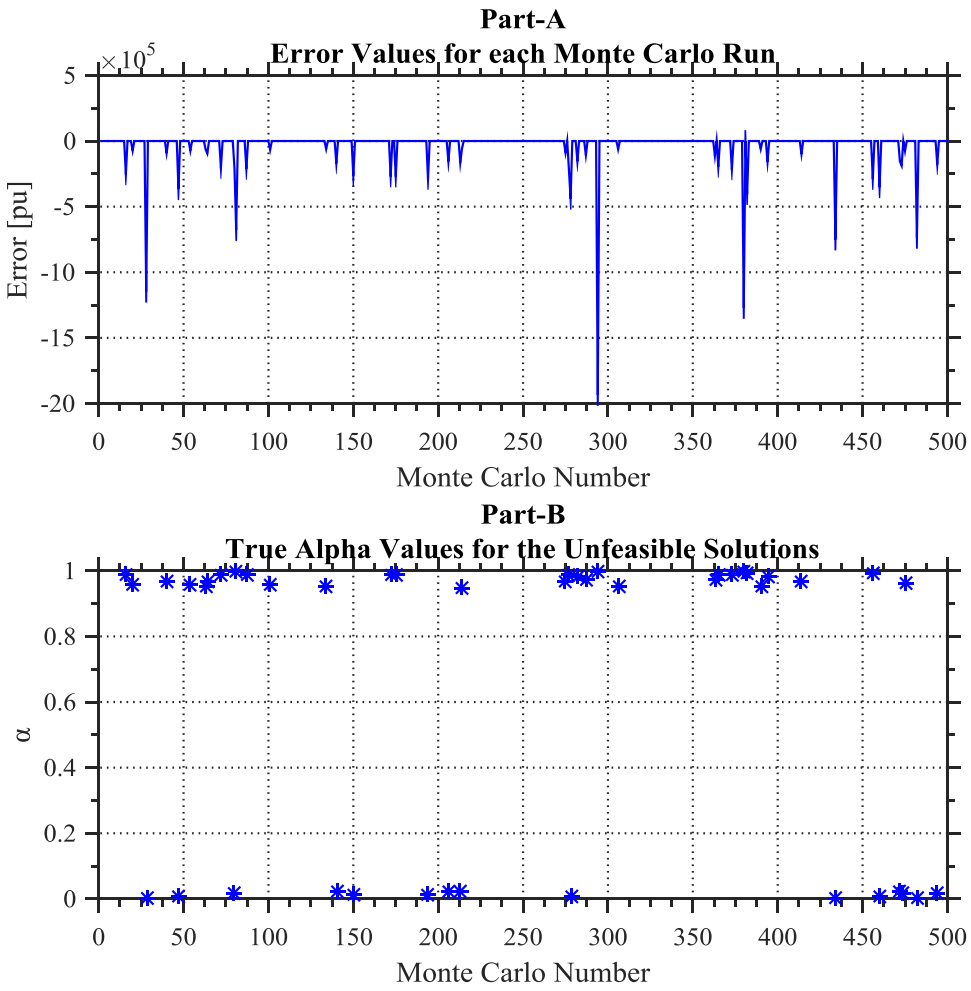

Figure 4-10 Error Between Estimated Location and Real Location for $\alpha_0 = 0.05$

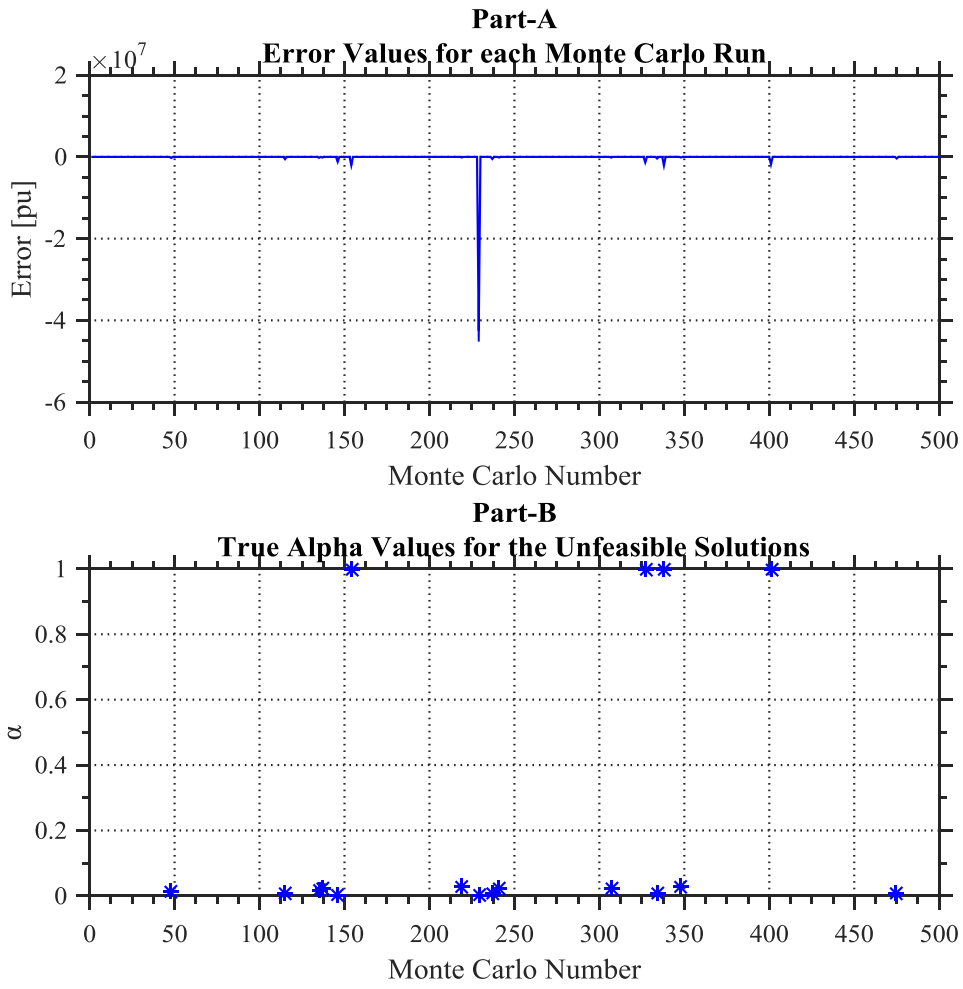

Figure 4-11 Error Between Estimated Location and Real Location for $\alpha_0 = 0.99$

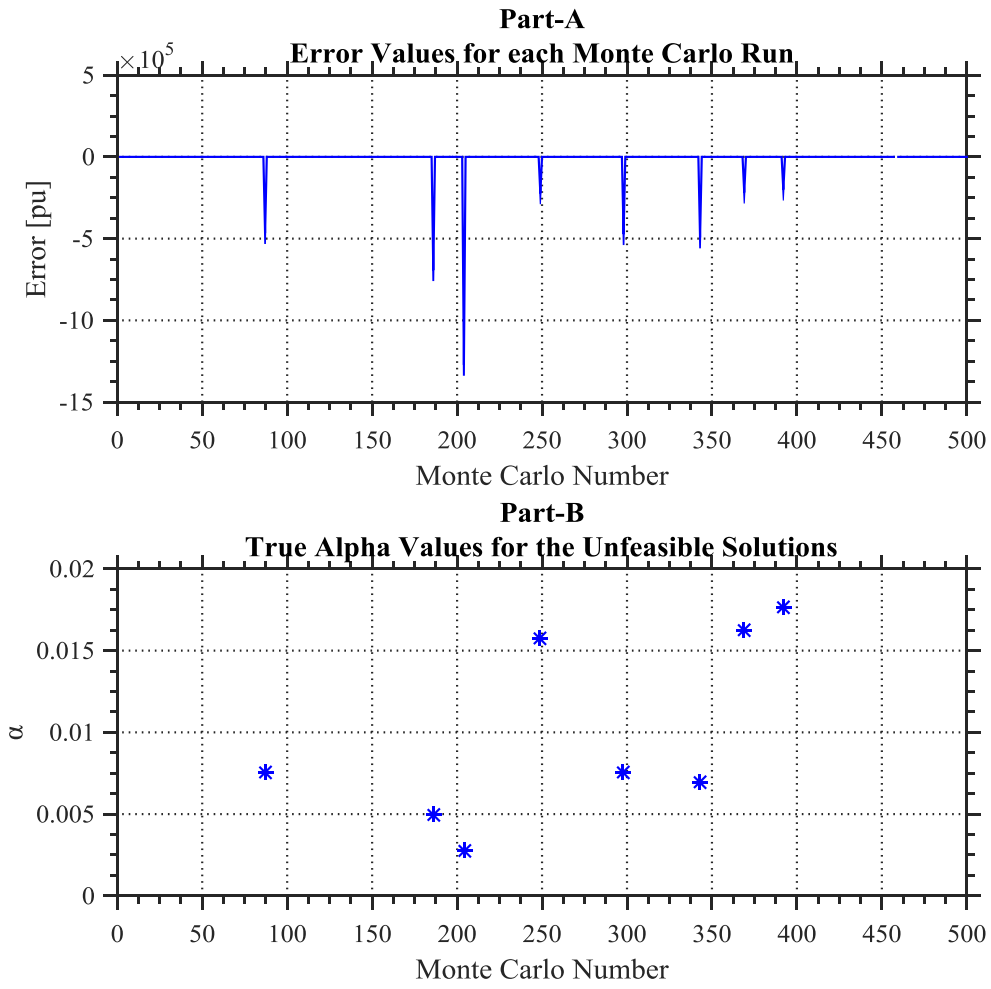

Figure 4-12 Error Between Estimated Location and Real Location for $\alpha_0 = 0.995$

Figure 4-7, Figure 4-8, Figure 4-9, Figure 4-10, Figure 4-11 and Figure 4-12 consist of two parts, namely, Part-A and Part-B. Part-A demonstrates the difference (error) between estimated location and real location of the fault for each Monte Carlo run. Part-B demonstrates the actual α values for the unfeasible solutions. Part-B of Figure 4-7, Figure 4-8, Figure 4-9, Figure 4-10, Figure 4-11 and Figure 4-12 depict that unfeasible solutions satisfies the condition (3.15) and (3.16). Since α_0 value is

selected as too close to 0 or too close to 1, unfeasible solutions indicate that the fault is located either at sending or receiving end.

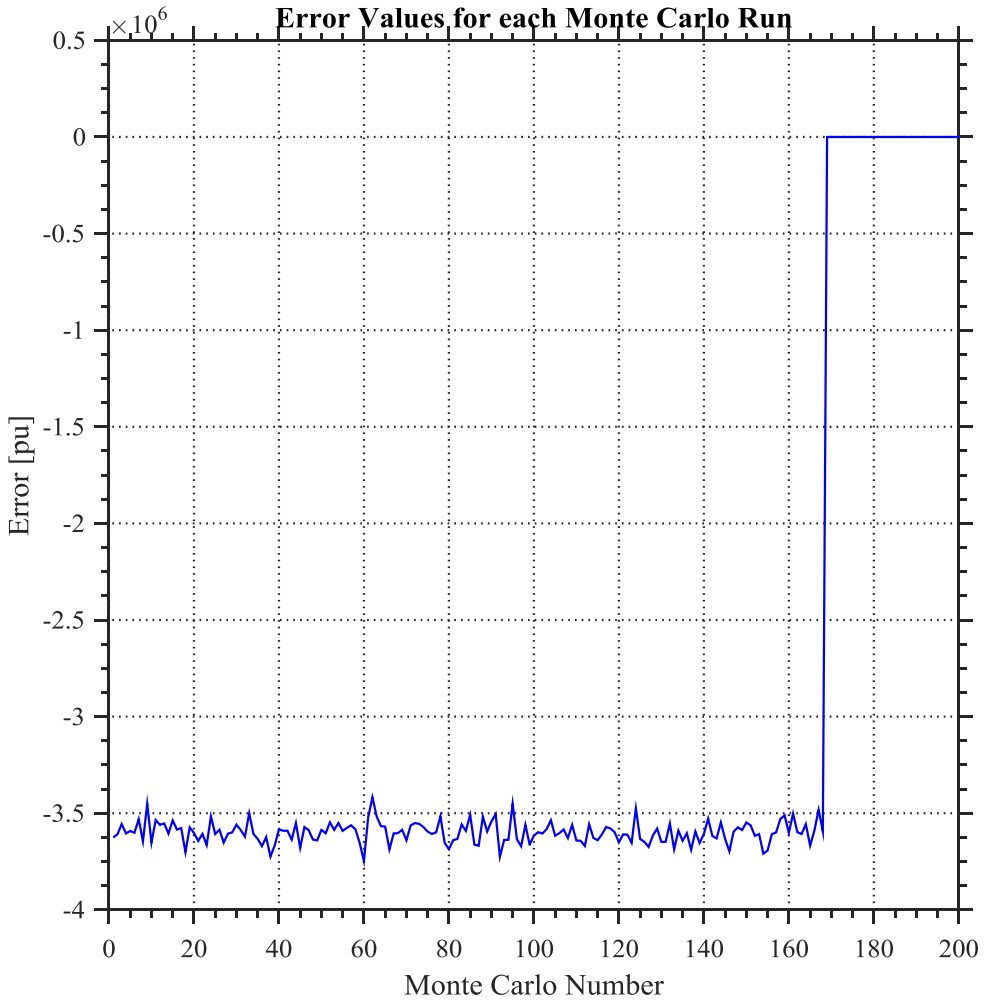

Figure 4-13 Error Between Estimated Location and Real Location for varied α_0

Finally in this section, it is shown that using a different α_0 will enable convergence to the feasible solution. For this purpose, a constant α value, 0.9992, is used instead of changing it randomly. In the first 100 Monte Carlo runs, the value of α_0 changes from 0.0001 to 0.01 with the step increase of 0.0001 and in the last 100 Monte Carlo

run, the value of α_0 changes from 0.99 to 0.9999 with the step increase of 0.0001. Figure 4-13 shows that after 169th Monte Carlo run whose corresponding α_0 value is 0.9968, the fault location problem is solved successfully. The pMAE is found to be 0.0309%. However, before the 168th Monte Carlo run, the solution is unfeasible. This result shows that, once the unfeasible solution is encountered, a different α_0 should be employed and estimation should be re-performed. As mentioned formerly, thanks to the small size of the estimation problem, this extra step will not bring a significant computational load.

4.3 Effect of Incorrect Line Parameters on the Proposed Method

Due to the varying weather conditions, the line parameters are subject to change. This section aims to validate even in the presence of incorrect line parameters, the proposed method is capable of locating faults correctly. In order to have such robustness against the incorrect line parameters, the problem formulation should be modified.

The equations (4.2) and (4.3) can be derived using (3.10) and (3.11) respectively.

$$I_{fi}\alpha Z = V_i - V_f + V_i b_{ii}\alpha^2 Z \tag{4.2}$$

$$I_{fj}(1-\alpha)Z = V_j - V_f + V_j b_{jj}(1-\alpha)^2 Z \tag{4.3}$$

where V_i, V_j and V_f are the voltage phasors at Bus-i, Bus-j and the fault location, respectively. Fault current flowing through Bus-i is represented by I_{fi}, while fault current flowing through Bus-j is represented by I_{fj}. Z represents the series impedance of the line between buses i and j, and b_{ii} and b_{jj} represent the line charging susceptances at Bus-i and Bus-j, respectively. Finally, α shows the ratio of the distance of the fault to Bus-i to the total length of the faulted line.

V_f is calculated for each equations, (4.2) and (4.3), shown in (4.4) and (4.5).

$$V_f = V_i - I_{fi}\alpha Z + V_i b_{ii}\alpha^2 Z \tag{4.4}$$

$$V_f = V_j - I_{fj}(1-\alpha)Z + V_j b_{jj}(1-\alpha)^2 Z \tag{4.5}$$

The equation (4.6) is derived using both equations, (4.4) and (4.5).

$$V_i - I_{fi}\alpha Z + V_i b_{ii}\alpha^2 Z = V_j - I_{fj}(1-\alpha)Z + V_j b_{jj}(1-\alpha)^2 Z \tag{4.6}$$

Finally, (4.7) is derived using the equation (4.6).

$$\alpha^2\left(V_i b_{ii} Z - V_j b_{jj} Z\right) + \alpha\left(-I_{fi}Z - I_{fj}Z + 2V_j b_{jj} Z\right) + V_i - V_j + I_{fj}Z - V_j b_{jj} Z = 0 \tag{4.7}$$

As seen in (4.7), α and the line impedance, *Z*, has a non-linear relationship. To be able to find α properly using the given analytic relation, the line impedance, *Z*, should be known accurately. However, the proposed algorithm is capable of finding α even the value of *Z* is incorrect.

To be able to obtain the robustness against line parameter error, the proposed algorithm should be modified. It is proposed to include line parameters (branch resistance, branch reactance, shunt susceptance) as states to be estimated to the proposed formulation. Since the number of states is increased in the modified formulation, an increased number of observations are required. By using raw data of a single cycle of voltage and current to compute phasor values, instead of two-cycle-long data, the observation number available can be increased from two to four, which will be enough for the proposed modified formulation. The proposed modification can be seen following.

$$z_{modified} = h\left(x_{modified}\right) + e \tag{4.8}$$

where $z_{modified}$ is modified measurement vector,

$h(x_{modified})$ is modified system state vector,

and *e* is measurement error vector.

$$x_{modified}^{T} =$$

$$\begin{bmatrix} V_f^{r,1} & V_f^{r,2} & V_f^{r,3} & V_f^{r,4} & V_f^{i,1} & V_f^{i,2} & V_f^{i,3} & V_f^{i,4} & \alpha_1 & \alpha_2 & b_{ii} \\ g_{ij} & b_{ij} & V_s^{r,1} & V_r^{r,1} & V_s^{r,2} & V_r^{r,2} & V_s^{r,3} & V_r^{r,3} & V_s^{r,4} & V_r^{r,4} & V_s^{i,1} \\ & & V_r^{i,1} & V_s^{i,2} & V_r^{i,2} & V_s^{i,3} & V_r^{i,3} & V_s^{i,4} & V_r^{i,4} & & \end{bmatrix} \quad (4.9)$$

where,

- $V_f^{r,m}$ is the real part of the voltage phasor at the fault location at time instant-m,
- $V_f^{i,m}$ is the imaginary part of the voltage phasor at the fault location at time instant-m,
- α_1 is the ratio of the distance of the fault to sending end bus to the total length of the faulted line
- α_2 is the ratio of the distance of the fault to receiving end bus to the total length of the faulted line
- g_{ij} is the shunt conductance between sending end bus and receiving end bus,
- b_{ij} is the shunt susceptance between sending end bus and receiving end bus,
- b_{ii} is the half of the total line charging between sending end bus and receiving end bus,
- $V_s^{r,m}$ is the real part of the system state voltage of sending end bus at time instant-m,
- $V_r^{r,m}$ is the real part of the system state voltage of receiving end bus at time instant-m,
- $V_s^{i,m}$ is the imaginary part of the system state voltage of sending end bus at time instant-m,

- $V_s^{i,m}$ is the imaginary part of the system state voltage of receiving end bus at time instant-m,

$$z_{modified}^{T} = \begin{bmatrix} I_s^{r,1} & I_r^{r,1} & I_s^{r,2} & I_r^{r,2} & I_s^{r,3} & I_r^{r,3} & I_s^{r,4} & I_r^{r,4} & I_s^{i,1} & I_r^{i,1} & I_s^{i,2} & I_r^{i,2} \\ I_s^{i,3} & I_r^{i,3} & I_s^{i,4} & I_r^{i,4} & \alpha_1 + \alpha_2 & V_s^{r,1} & V_r^{r,1} & V_s^{r,2} & V_r^{r,2} & V_s^{r,3} & V_r^{r,3} \\ V_s^{r,4} & V_r^{r,4} & V_s^{i,1} & V_r^{i,1} & V_s^{i,2} & V_r^{i,2} & V_s^{i,3} & V_r^{i,3} & V_s^{i,4} & V_r^{i,4} \end{bmatrix} \quad (4.10)$$

where,

- $I_s^{r,m}$ is the real part of the measured current of sending end of the faulted line at time instant-m,
- $I_r^{r,m}$ is the real part of the measured current of receiving end of the faulted line at time instant-m,
- $I_s^{i,m}$ is the imaginary part of the measured current of sending end of the faulted line at time instant-m,
- $I_r^{i,m}$ is the imaginary part of the measured current of receiving end of the faulted line at time instant-m,
- α_1 is the ratio of the distance of the fault to sending end bus to the total length of the faulted line
- α_2 is the ratio of the distance of the fault to receiving end bus to the total length of the faulted line
- $V_s^{r,m}$ is the real part of the system sending end bus voltage at time instant-m,
- $V_r^{r,m}$ is the real part of the system receiving end bus voltage at time instant-m,
- $V_s^{i,m}$ is the imaginary part of the sending end bus voltage at time instant-m,

- $V_s^{i,m}$ is the imaginary part of the receiving end bus voltage at time instant-m,

The simulations are repeated 200 times by changing α randomly. In each run of algorithm, a three-phase to ground fault is located between the Bus-1 and Bus-2. The faulted line impedance, given in Table 4-2, is multiplied by a coefficient. The coefficient is chosen as 2 for the half of the Monte Carlo simulations and for the rest of the Monte Carlo simulations it is chosen as 0.5. The pMAE of the estimation values of α in all runs for different initial conditions are presented in Table 4-9.

Table 4-9 pMAE for Different Fault Location at a Given Line with incorrect impedance

α_0	**pMAE**
0.005	0.1473 %
0.01	0.0106 %
0.02	0.0339 %
0.05	0.0138 %
0.99	0.053 %
0.995	0.1541 %

The results in Table 4-9 are similar with the pMAEs of Table 4-8. This result validates the proposed method is capable of locating faults correctly, even in the presence of incorrect line parameters.

The performance of the algorithm for a fault between Bus-1 and Bus-2 can be seen in Figure 4-14. Figure 4-14 shows the error between estimated location and real location. All Monte Carlo runs are taken when the line parameters of the branch between Bus-1 and Bus-2 are doubled.

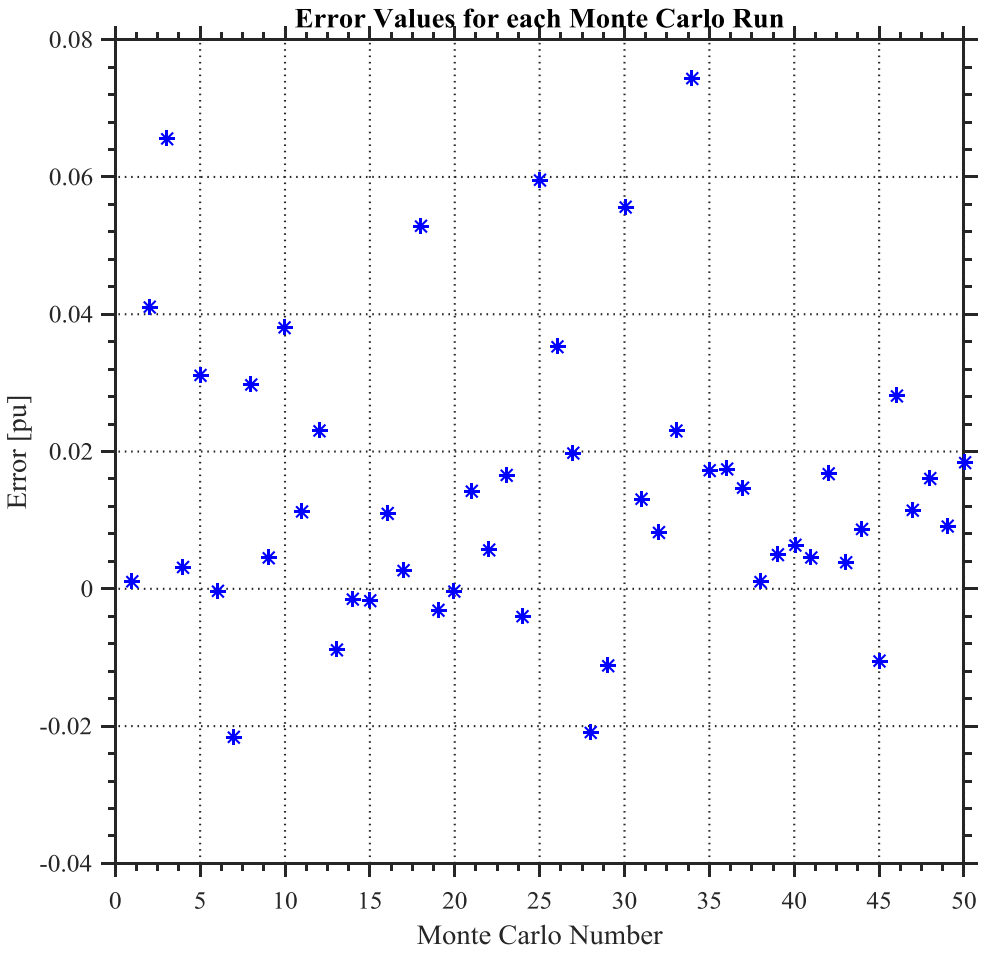

Figure 4-14: Error Between Estimated Location and Real Location with Incorrect Impedance

Figure 4-14 depicts that the estimated fault location is not affected under the incorrect line parameters.

4.4 Effect of Multiple Faults on the Proposed Method

This section aims to validate fault location with proposed method when there are multiple faults in the system. The faulted lines are selected between the Bus-1 and

Bus-2 and between Bus-6 and Bus-11. Then Monte-Carlo simulations are run 100 times by changing α of each faulted line randomly. The pMAE for each α is calculated and presented in Table 4-10.

Table 4-10 pMAE for a Given Fault Locations

Faulted Line	**pMAE (α_0 = 0.005)**
Between Bus-1 and Bus-2	0.0109 %
Between Bus-6 and Bus-11	0.001 %

4.5 Discussion

The simulations were performed in MATLAB environment by following the steps stated below.

- The IEEE 14-bus system is employed.
- Optimal PMU placement algorithm is run to be able to have an observable system.
- Power flow problem is solved to obtain the measurement set for the state estimator.
- Faulted line is found with state estimation and bad data process (Normalized Residual Test).
- Fault location is determined with WLS.
- MAEs of estimated values of fault location are found with Monte Carlo analysis.

Simulation results demonstrate that

- The proposed method can identify faulted lines successfully.

- The proposed approach can locate a fault on an identified faulted line accurately.
- Initial condition, α_0, is critical because of the risk of unfeasible solution.
- Using small α_0 values can solve the unfeasible solution problem.
- Small α_0 values might increase the iteration of the solution.
- When small size of the problem is considered, the increased number of iterations will not create a significant change in the total solution time of the problem.
- Even the fault line impedance is incorrect, the proposed algorithm can handle this situation and finds fault location accurately.
- The proposed algorithm is capable of locating multiple faults.

CHAPTER 5

CONCLUSION

Fault location is especially important for the restoration of electrical power, which will increase the reliability of the system and decrease the operational cost. The main motivation of this thesis work was to locate a permanent fault with a technique based on the well-known WLS state estimation method.

The method assumes that the considered system is observable solely by PMUs considering their increasing number. The high refresh rate and time synchronization of the PMU measurements is the reason of using those data for the proposed method. Note that, the proposed method is applicable to any synchronized data set that may be received from PMUs or power quality monitors. The contributions of the proposed method can be listed as follows.

- The state estimation based method uses multiple time scans to increase the accuracy of the fault location, and to eliminate the measurement redundancy problem.
- The proposed faulted line identification is actually a part of conventional state estimation, and hence will not bring any computational burden. Thanks to the local problem formulation, the computational burden of the fault location on a transmission line is negligible.

- During simulations it was observed that the initial condition of the estimation problem is critical, because of the risk of unfeasible solution. Therefore, it is proposed to use small α_0 values to initialize the problem. This choice might increase the iterations of the solution, but considering the small size of the problem, the increased number of iterations will not create a significant change in the total solution time of the problem.
- The proposed faulted line identification method is capable of identifying multiple faulted lines in the system.
- The proposed fault location method is capable of eliminating the effect of incorrect line parameters, which brings robustness against the parameter changes due to weather conditions.
- In this thesis work, all relations are derived for three-phase to ground fault. However, if a three-phase estimator is employed, the proposed fault location method can be applied independent of the fault type.

In the future, it is aimed to apply the proposed method using real time synchronized PMU measurements.

REFERENCES

[1] S. Santoso, A. Gaikwad and M. Patel, “Impedance-Based Fault Location in Transmission Networks: Theory and Application,” IEEE Access, vol. 2, pp. 537-557, 2014.

[2] T. Takagi, Y. Yamakoshi, M. Yamaura, R. Kondow, and T. Matsushima, “Development of a new type fault locator using the one-terminal voltage and current data,” IEEE Trans. Power App. Syst., vol. PAS-101, no. 8, pp. 2892–2898, Aug. 1982.

[3] L. Eriksson, M. M. Saha, and G. D. Rockefeller, “An accurate fault locator with compensation for apparent reactance in the fault resistance resulting from remore-end infeed,” IEEE Trans. Power App. Syst., vol. PAS-104, no. 2, pp. 423–436, Feb. 1985.

[4] T. Kawady and J. Stenzel, “A practical fault location approach for double circuit transmission lines using single end data,” IEEE Trans. Power Del., vol. 18, no. 4, pp. 1166–1173, Oct. 2003.

[5] C. E. M. Pereira and L. C. Zanetta, Jr., “Fault location in transmission lines using one-terminal postfault voltage data,” IEEE Trans. Power Del., vol. 19, no. 2, pp. 570–575, Apr. 2004.

[6] M. Kezunovic and B. Perunicic, “Automated transmission line fault analysis using synchronized sampling at two ends,” IEEE Trans. Power Syst., vol. 11, no. 1, pp. 441–447, Feb. 1996.

[7] A. L. Dalcastagnê, S. N. Filho, H. H. Zürn, and R. Seara, “An iterative two-terminal fault-location method based on unsynchronized phasors,” IEEE Trans. Power Del., vol. 23, no. 4, pp. 2318–2329, Oct. 2008.

[8] Y. Liao and N. Kang, “Fault-location algorithms without utilizing line parameters based on the distributed parameter line model,” IEEE Trans. Power Del., vol. 24, no. 2, pp. 579–584, Apr. 2009.

[9] J. Izykowski, E. Rosolowski, P. Balcerek, M. Fulczyk, and M. M. Saha, “Accurate noniterative fault location algorithm utilizing two-end unsynchronized measurements,” IEEE Trans. Power Del., vol. 25, no. 1, pp. 72–80, Jan. 2010.

[10] C. A. Apostolopoulos and G. N. Korres, “A novel algorithm for locating faults on transposed/untransposed transmission lines without utilizing line parameters,” IEEE Trans. Power Del., vol. 25, no. 4, pp. 2328–2338, Oct. 2010.

[11] T. Nagasawa, M. Abe, N. Otsuzuki, T. Emura, Y. Jikihara, and M. Takeuchi, “Development of a new fault location algorithm for multiterminal two parallel transmission lines,” IEEE Trans. Power Del., vol. 7, no. 3, pp. 1516–1532, Jul. 1992.

[12] D. A. Tziouvaras, J. B. Roberts, and G. Benmouyal, “New multi-ended fault location design for two- or three-terminal lines,” in Proc. 7th Int. Conf. Develop. Power Syst. Protection, 2001, pp. 395–398.

[13] G. Manassero, E. C. Senger, R. M. Nakagomi, E. L. Pellini, and E. C. N. Rodrigues, “Fault-location system for multiterminal transmission lines,” IEEE Trans. Power Del., vol. 25, no. 3, pp. 1418–1426, Jul. 2010.

[14] T. Funabashi, H. Otoguro, Y. Mizuma, L. Dube, and A. Ametani, “Digital fault location for parallel double-circuit multi-terminal transmission lines,” IEEE Trans. Power Del., vol. 15, no. 2, pp. 531–537, Apr. 2000.

[15] S. M. Brahma, “Fault location scheme for a multi-terminal transmission line using synchronized voltage measurements,” IEEE Trans. Power Del., vol. 20, no. 2, pp. 1325–1331, Apr. 2005.

[16] C.-W. Liu, K.-P. Lien, C.-S. Chen, and J.-A. Jiang, “A universal fault location technique for N-terminal transmission lines,” IEEE Trans. Power Del., vol. 23, no. 3, pp. 1366–1373, Jul. 2008.

[17] S. Rajendra and P. G. McLaren, “Travelling-wave techniques applied to the protection of teed circuits: Multi-phase/multi-circuit system,” IEEE Trans. Power App. Syst., vol. PAS-104, no. 12, pp. 3551–3557, Dec. 1985.

[18] A. O. Ibe and B. J. Cory, “A travelling wave-based fault locator for two- and three-terminal networks,” IEEE Trans. Power Del., vol. 1, no. 2, pp. 283–288, Apr. 1986.

[19] F. H. Magnago and A. Abur, “Fault location using wavelets,” IEEE Trans. Power Del., vol. 13, no. 4, pp. 1475–1480, Oct. 1998.

[20] C. Y. Evrenosoglu and A. Abur, “Travelling wave based fault location for teed circuits,” IEEE Trans. Power Del., vol. 20, no. 2, pp. 1115–1121, Apr. 2005.

[21] D. Spoor and J. G. Zhu, “Improved single-ended traveling-wave fault location algorithm based on experience with conventional substation transducers,” IEEE Trans. Power Del., vol. 21, no. 3, pp. 1714–1720, Jul. 2006.

[22] P. Jafarian and M. Sanaye-Pasand, “A traveling-wave-based protection technique using wavelet/PCA analysis,” IEEE Trans. Power Del., vol. 25, no. 2, pp. 588–599, Apr. 2010.

[23] M. Korkali and A. Abur, “Fault location in meshed power networks using synchronized measurements,” in Proc. North American Power Symp., Sep. 2010.

[24] M. Korkali, H. Lev-Ari and A. Abur, “Traveling-Wave-Based Fault-Location Technique for Transmission Grids Via Wide-Area Synchronized Voltage Measurements,” IEEE Trans. Power Sys., vol. 27, no. 2, pp. 1003–1011, May 2012.

[25] Volkan Özdemir, “A Local Parameter Estimator Based on Robust LAV Estimation,” MS Thesis, Middle East Technical University, 2015.

[26] A. G. Phadke, J. S. Thorp, “Synchronized Phasor Measurements and Their Applications”, book, Springer, 2008.

[27] A. Abur and A. Gomez-Exposito, “Power System State Estimation: Theory and Implementation”, Marcel Dekker, 2004.

[28] A. Akyel, “Detemination of Dynamic Problems Associated with the Wind Power Plants in Turkish Transmission System,” MS Thesis, Middle East Technical University, 2015.

[29] M. Shiroei, S. Daniar and M. Akhbari, “A new algorithm for fault location on transmission lines”, in proc. IEEE Power & Energy Society General Meeting, 2009, pp. 1-5.

[30] A. C. Aitken, “On Least Squares and Linear Combinations of Observations”, Proc. Royal Society of Edinburg, 1935, vol. 35, pp. 42-48.

[31] M. Göl, A. Abur. “Optimal PMU Placement for State Estimation Robustness,” IEEE Innovative Smart Grid Technologies (ISGT) Europe, Oct. 2014.

[32] A. Monticelli and A. Garcia, “Reliable Bad Data Processing for Real-Time State Estimation,” IEEE Transactions on Power Apparatus and Systems, Vol. PAS-102, No. 5, May 1983, pp. 1126-1139.